Dr. Billings

NATURAL AND EXPERIMENTAL WEATHERING OF BASALTS

A Dissertation

Presented to the Graduate Faculty of the

New Mexico Institute of Mining and Technology

In Partial Fulfillment

of the Requirements for the Degree

Doctor of Philosophy

in Geoscience

by

Haia Lifshitz-Roffman

October 1971

TABLE OF CONTENTS

	Page
LIST OF FIGURES	iv
LIST OF TABLES	v
ABSTRACT	vii
ACKNOWLEDGEMENTS	viii
INTRODUCTION	1
LITERATURE	1
Natural weathering of rocks and minerals	1
Weathering of basalts	2
Experimental weathering of minerals	3
Experimental alteration of glasses	3
Experimental weathering of basalts	4
NATURAL WEATHERING OF NEW MEXICO BASALTS	5
Samples	5
Present and past climates	7
Age of flows	7
Quantitative mineralogy	9
Chemical observations	18
Summary and conclusions	27
EXPERIMENTAL WEATHERING	29
Introduction	29
Sample preparation	29
Column leaching experiments	30

Page

A column evaporation experiment 32

Short term leaching experiments 33

Long term leaching experiments. 42

Experiments of alternate wetting and drying 48

Summary and conclusions 57

GEOCHEMICAL CONSIDERATIONS 59

Correlation between experimental and natural weathering 59

Plagioclase weathering 61

Caliche formations 62

Origin of the Santo Tomas-Black Mountain flows . . 64

SUMMARY 67

PLATES 69

APPENDIX A: ANALYTICAL PROCEDURES 79

APPENDIX B: MINERALOGICAL AND CHEMICAL RESULTS 90

APPENDIX C: APPARATUS FOR ALTERNATE WETTING AND DRYING EXPERIMENTS 111

REFERENCES 114

LIST OF FIGURES

Figure Number	Title	Page
1	Index Map of the Potrillo volcanics	6
2	Histogram of WI_{Fe} for the Santo Tomas flows	14
3	Histogram of WI_{Fe} for the San Miguel and Black Mountain-6 flows	15
4	Effect of weathering time on ΔWI_{Fe} . . .	16
5	Altered layer thickness	17
6	Change in iron with weathering time . . .	24
7	Jenny's weathering index	25
8	Parker's modified weathering index	25
9	Basalt weathering solution	35
10	Grain size effect on basalt weathering solution	36
11	Rate of attainment of stable conductivity .	37
12	Results of basalt long term leaching experiments	47
13	Chemical composition of basalt wash solutions versus accumulative experimental time .	51
14	Chemical composition of glass wash solutions versus accumulative experimental time .	53
15	Schematic diagram of the water system .	112
16	Schematic diagram of the electronic circuit	113

LIST OF TABLES

Table Number	Title	Page
1	Radiometric ages of flows	8
2	Age assignment	8
3	Mean mineralogical composition of flows: including vesicles	12
4	Mean mineralogical composition of flows: excluding vesicles	12
5	Average chemical changes between weathered and nonweathered portion of the flows . . .	20
6	Iron weathering indeces	22
7	Chemical composition of minerals and glass used in experimental weathering . .	31
8	Results of short term leaching of minerals and glass	41
9	Analysis of filtrate from run 6	43
10	Relative mobility of cations from run 6 . .	43
11	Chemical analyses of basalt standards . .	82
12	X-ray fluorescence instrumental parameters	83
13	X-ray fluorescence instrumental precision	84
14	Atomic absorption instrumental parameters	87
15	Analyses of 10x concentrated standard solution by evaporation and by an ion exchanger	89
16	Mineralogical composition of flows	91

Table Number	Title	Page
17	Chemical analysis of flows	101
18	Chemical analysis of short term leaching experiments	104
19	Concentration of washing solutions of alternate wetting and drying experiments	107
20	X-ray data for calcite.	110

ABSTRACT

Fresh and weathered parts of five basalt flows from south-central New Mexico have been investigated in the natural part of this study. In the weathered parts, an iron bearing phase (Fe-mineral) that increases quantitatively with time has been observed. This phase led to the definition of a very useful weathering index.

$$WI_{Fe} = \frac{100 \times (\text{Fe-mineral})}{100 - (\text{Plag} + \text{Vs} + \text{Fe-mineral})}$$

The change in the total iron concentration ($\Delta \leq Fe$), the change in the ferrous to ferric concentrations ($\Delta(Fe^{+2}/Fe^{+3})$), Jenny's weathering index and the herein modified Parker weathering index as well as WI_{Fe} have been proven to be most suitable in measuring the degree of weathering of basalts located in dry environments.

Five types of weathering experiments were carried out using a basalt, a glass of basaltic composition and the basalt minerals. These experiments indicate that the mechanism of weathering is composed of two steps: a rapid reaction of leaching that takes place as the sample comes in touch with the weathering solution and the slow process of diffusion that follows. Experiments simulating weathering in moist areas suggest the formation of gibbsite. Weathering in desert areas is best simulated by experiments of alternate wetting and drying, and results in the developing of calcite, Mg-montmorillonite sepiolite, attapulgite, and iron oxyhydroxides.

ACKNOWLEDGMENTS

I wish to express my gratitude to my advisory committee: Drs. Gale Billings, Charles Chapin, Wayne Ohline, and Jacques Renault for their guidance, advice and many helpful discussions that led to the completion of this study. I am grateful to Mr. Don H. Baker, Jr., Director of the New Mexico State Bureau of Mines and Mineral Resources for supporting this research and for his advice and useful comments.

I am thankful to Dr. Robert Weber for the gem quality augite and olivine used in this research, to Mrs. Lynn Brandvold and her staff for chemical analysis of samples, to Mr. Charles Walker for scanning electron microscope photographs and to Drs. Kay Brower and Gerardo Gross for the use of their facilities. I greatly appreciate the technical help given by staff members of the New Mexico State Bureau of Mines and Mineral Resources. Special thanks are due to Dr. John Hawley, Geologist U. S. Soil Conservation Service, for assisting in sampling the basalt flows and for information on the general geology of the area.

This dissertation would have never been done without the encouragement, love and understanding of my parents, my husband and my son.

INTRODUCTION

The primary purpose of this study was to determine the results of natural weathering in arid climates, and to simulate this process for various climates by laboratory experiments.

If a rate dependent weathering function for basalts could be defined for specified conditions, relative ages could then be assigned. This might prove to be as beneficial and considerably less-costly than radioactive age measurements. In more recent rocks, it might even prove as precise. The rate dependent parameters might be a newly created phase, a decrease in an old phase, or an alteration in elemental ratios.

Attempts to establish the rate and process of weathering have been made in this dissertation by studying:

(a) chemical and mineralogical changes that occur during natural weathering of basalts

(b) chemical and mineralogical changes that occur in experimental weathering of basalts and basalt components; e. g. glass and minerals.

LITERATURE

Natural Weathering of Rocks and Minerals

Goldich (1938) in his comprehensive study of weathering of a variety of rocks has established the basic sequence of relative weatherability of igneous rock-forming mineral:

olivine > augite > hornblende > biotite, and

Ca-plagioclase > Na-plagioclase > K-feldspar > quartz

and called this concept: The stability principle. Many investigators confirmed Goldich's stability principle (Aomine and Wada, 1962; Wolff, 1967; McLaughlin, 1955; Craig and Laughnan, 1964).

The relative mobility of ions under natural conditions has been listed by Smyth (1913) and Polynov (1937) to be the following sequence: Ca > Na > Mg > K > Si > Al = Fe. Anderson and Hawkes (1958) examining the stream water and granitic rocks found a slightly different sequence: Mg > Ca > Na > K > Si > Al = Fe.

Dennen and Anderson (1962) studied chemical changes in the weathering crust of 32 rocks. Early stages of weathering were indicated by the oxidation of ferrous iron followed by the removal of the soluble ions Na^{+}, Ca^{+2} and Mg^{+2}. The concentration of the oxidized iron in the form of hematite, maghemite and/or goethite was also noticed by: Sherman (1952), Craig and Laughnan (1964) and Augusthitis and Ottemann (1966).

Weathering of Basalts

All investigations known to the author of weathering of basalts were made on rocks located in moist regions: Hawaiian Islands, Northern Ireland and New South Wales.

Bates (1962) studied weathered Hawaiian basalts and found that in moderate leaching areas, the products are serpentine, trioctahedral montmorillonite, various ferric hydrates and gels, halloysite and

allophane. Where leaching was optimum gibbsite and amorphous alumina and ferric hydrates formed. Sherman (1949), 1952b) suggested that the controlling factor of weathering is not the total rainfall, but its distribution. Where a dry period exists, weathering enriches the horizon in ferric and titanium oxides, in the absence of such a dry period bauxite is the dominant consituent. The importance of dry periods was also noted by Hay and Jones (in press). The same processes are apparent in moist climates of Ireland and New South Wales (Eyles, 1952; Craig and Laughnan, 1964; Laughnan and Bayliss, 1963).

Experimental Weathering of Minerals

The most important studies concerning experimental weathering of minerals were reported by: Norton (1941), Graham (1949), Morey and Chen (1955), Wollast (1957), De Vore (1958), Reesman and Keller (1958), Correns (1961), Manning (1965) and Huang and Keller (1970). The pertinent works of these authors will be discussed in later portions of this dissertation.

Experimental Alteration of Glasses

Glass is a major component of basalt. This amorphous silicate plays a very important part in the total weathering of basalts. Glasses have been studied mainly by ceramic engineers and oceanographers. The most important works that are and can be applied to weathering were reported by: Hawser and Raynolds (1939), Lyle (1943), Swift

(1947), Johnson et al. (1951), Friedman et al. (1966), Douglas and El-Shamy (1967), Noble (1967), Lofgren (1970) and Burkett (1970). The pertinent works of these authors will be discussed in later parts of this dissertation.

Experimental Weathering of Basalts

Pedro (1961) and Pedro and Hemin (1964) have demonstrated laboratory weathering under humid tropical conditions. They reported leaching fragments in vertical columns with recycled, hot (70°C) distilled water. Over a period of two years two layers developed on the leached rocks: (1) an upper "atmospheric zone" and (2) a saturated "fluctuating water table" zone. In the "atmospheric zone" a crust of bohemite, hematite and limonite formed, and in the "fluctuating water table" zone gibbsite formed. The leach solution contained silica, alkalies, alkaline-earths and some alumina.

NATURAL WEATHERING OF NEW MEXICO BASALTS

Samples

Parts of the Santo Tomas-Black Mountain basalts located in south-central New Mexico have been chosen for the portion of this investigation concerning natural weathering (Figure 1). The three Santo Tomas flows, (1, 2, 3) the San Miguel and the youngest of the Black Mountain flows (flow number 6) were selected for this study because they are located close to each other or even one on top of the other (Santo Tomas flows), which provides them with similar climates or even microclimates.

No flow from a given center coalesces with those of the neighboring centers. Kottlowski (1960), Hawley (1965) and Hawley and Kottlowski (1969), have described the area. Hoffer (1969, 1971) studied the mineralogy of these flows and classified them according to their phenocryst composition. The sampling and sample designation are based on the maps and flow numbers of Hoffer (1969). Samples were selected to be as near as possible to those radiometrically dated by the Field Research Laboratory (discussed later). Samples averaged 0.25 cubic feet in size. They were collected from the flow surface but free from soil and vegetation. From the Santo Tomas-1 flow twelve samples were collected, from Santo Tomas-2 ten, from Santo Tomas-3 ten, from San Miguel six and from Black Mountain-6 six samples were collected.

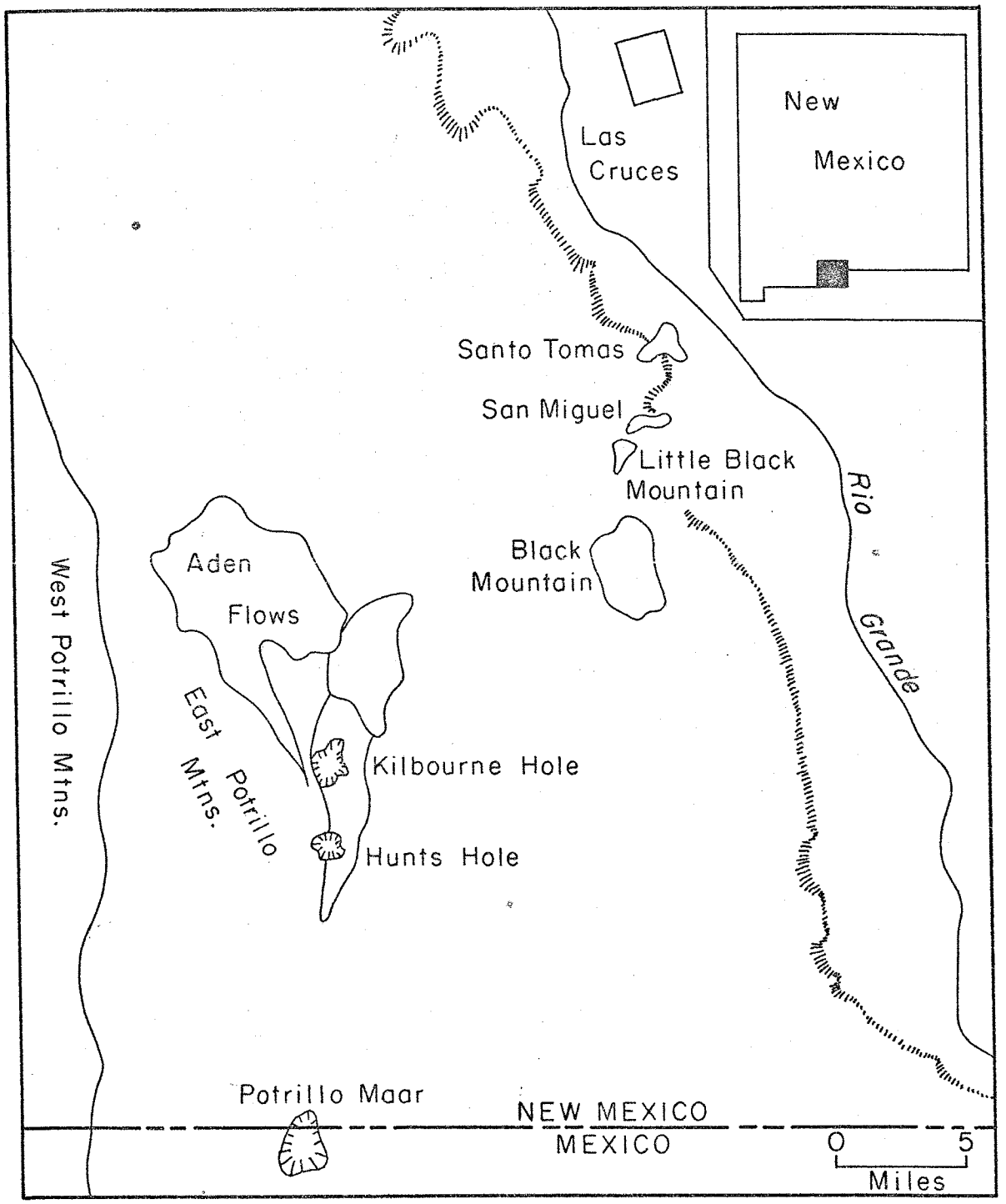

FIGURE 1
Index map of the Potrillo Volcanics
(After Hoffer, 1969)

Present and Past Climates

The present climate in the studied area is arid to semi-arid. Summer temperatures are high, and the day-night temperature differences are high also. Most precipitation in the area is rain. The average annual rainfall in the last 120 years was 8-10 inches (Reynolds, 1956, King et al. 1970). The humidity in the area is low; the average humidity in the early morning hours is about 60%, and is less than 30% during warmer periods (weather Bureau, 1962).

Paleobottanic evidence (Kottlowski 1958, Martin 1964, Martin and Metringer 1965, and Gile 1966), indicates that the area has been under glacial influence in the Pleistocene. The Pleistocene pluvial climates differed from the present climate in having higher precipitation and lower temperatures. Pollen analysis suggest that the average annual rainfall when under glacial influence has not exceeded twice the average present precipitation. Rainfall of 16-20 inches and lower average temperatures than in the present suggests no major change in rate of weathering for the studied flows from time of extrusion to present.

Age of Flows

The studied flows have been radiometrically dated several times, as listed in Table 1. The dates reported recently by the Field Research Laboratory (FRL) agree best with the stratigraphy and the topography of the area and are used here.

TABLE 1

Radiometric Ages* of Flows

Flow	A	B	C
San Miguel	1.84 ± 0.5		0.150 ± 0.116 0.226 ± 0.078
Santo Tomas - 1	8.5 ± 0.5	2.65 ± 0.35	0.161 ± 0.077 0.127 ± 0.127
Santo Tomas - 2		2.35 ± 0.2	0.040 ± 0.133 0.116 ± 0.116
Black Mountain - 6	1.69 ± 0.15		0.025 ± 0.100 0.126 ± 0.102

* Age in millions of years

A. By geochron Laboratories Inc. of Cambridge Massachusetts, (Hawley, 1967)

B. By Geochron Laboratories (Hoffer, 1969)

C. By Field Research Laboratory - Mobil Research and Development Corporation, Dallas Texas, 1970

TABLE 2

Age Assignment*

Flow	Age
San Miguel	180,000
Santo Tomas - 1	150,000
Santo Tomas - 2	100,000
Santo Tomas - 3	75,000
Black Mountain - 6	50,000

* See text for explanation

The difficulty in dating radiometrically such young basalts, is well expressed by the high standard deviation that appears in Table 1. The various weathering indicies of this dissertation may help establish more reliable and less costly age-dating methods. For this purpose, it is necessary to assign approximate ages for the studied flows. Using for the FRL ages, the probability formula (Burington and May, 1958):

$$\frac{(A\pm a) + (B\pm b)}{2} = \frac{A+B}{2} \pm \sqrt{\frac{a^2+b^2}{2}}$$

and considering geological observations, the ages listed in Table 2 have been assigned by the writer. Should one or several of the weathering indicies behave differently than the others with respect to weathering time, it will prove an error in assigned sequence or values. But should all the weathering indicies behave in the same manner with respect to weathering time, they will strongly verify the assigned ages.

Quantitative Mineralogy

The inspected flows are porphiritic hypocrystalline in texture and composed of the following primary constituents: plagioclase, olivine, pyroxene (augite), magnetite, glass, iddingsite and vesicles, and the secondary minerals: calcite, opal and an identifiable Fe-mineral.

Fe-mineral is important to weathering investigations. It occurs on the weathered surface and close to vesicles, especially those filled with calcite as small brownish - reddish nonpleochroic

grains. The small size (< 0.02 mm) makes it impossible to separate them from the total groundmass for accurate identification purposes. An x-ray diffraction pattern of a weathered surface containing a relatively high amount of this mineral (Santo Tomas-1) did not reveal the presence of any mineral except the major constituents of the basalt. The difficulty in identifying this material was mainly due to the relatively small concentration present in these young flows.

In older basalts this species is present in higher quantities. The basalts, Seldon A and Seldon B, located in the Rio Grande Valley (T20S, R1W) 12 miles northwest of Las Cruces were reported to be 9.3 million years old by the Field Research Laboratory. They were sampled because of large amounts of the Fe-mineral. An x-ray diffraction pattern of these basalts showed the three major goethite peaks. Goethite is also a constituent in iddingsite (Sun, 1957), but it is very unlikely that the peaks appearing on the Seldon Basalt chart belong to iddingsite, since iddingsite showed goethite peaks only when exposed to x-rays for many hours using the film technique. It is reasonable to assume that goethite is one (or the major) constituent of this species. The fact that iron is enriched in the weathered surface (Table 17 Appendix B) the color and the x-ray analyses indicate that these grains are iron rich and therefore will be called Fe-mineral. This assumes that this iron rich phase is a mineral although diagnostic characteristics have not been recognized other than the appearance of some goethite x-ray peaks.

The mineralogical composition of the five selected flows was determined by point counting (Table 16 Appendix B) as described in Appendix A. The reproducibility was best when augite magnetite and glass were reported together. The reproducibility of the point counting was established by techniques given in Appendix A.

In point counting the weathered rock it was impossible to tell whether an indentation on the thin section was a vesicle or not. For this reason mineralogical compositions are based on percentages excluding vesicles or potential vesicles (Table 4).

The main mineralogical changes that take place as a result of weathering are: decrease in the amount of glass + augite + magnetite, olivine and plagioclase (as indicated in Table 4). The relatively high loss in the first is mainly due to the comparatively quicker decomposition of the metastable glass. The only increase is in the amount of the iron-rich mineral. In essence, the iron leaches out of the primary minerals but because it is not within a flowing water solution, it precipitates to form the Fe-mineral. The relative amount of this mineral is expressed as:

$$WI_{Fe} = \frac{100 \times \text{Fe-mineral}}{100 - (\text{plag} + \text{Vs} + \text{Fe-mineral})}$$

Student's t test was calculated for every weathered and nonweathered population of each flow, and in every case the number of thin section point counted exceeded the required number of samples for the mean composition of WI_{Fe} to be within 95 percent confidence (for technique

TABLE 3

Mean Mineralogical Composition of Flows

Including Vesicles

Flow		%Vs	%Plag.	%Ol	%Gl+Au +Mag	%Idd	%Fe-min.
San Miguel	$1\bar{n}$	11.03	36.09	12.55	38.74	1.01	0.60
	$\bar{w}$	1.67	39.12	12.54	40.58	1.71	4.45
Santo Tomas	$1\bar{n}$	3.77	32.70	9.16	54.13	0.00	0.25
	$\bar{w}$	0.71	32.93	9.19	52.83	0.00	4.35
Santo Tomas	$2\bar{n}$	6.44	31.17	9.67	52.52	0.05	0.15
	$\bar{w}$	1.62	32.64	9.63	52.92	0.10	3.10
Santo Tomas	$3\bar{n}$	14.37	28.13	10.23	46.99	0.10	0.15
	$\bar{w}$	1.81	30.30	10.98	53.61	0.67	2.64
Black Mountain	$6\bar{n}$	13.60	36.46	10.79	38.91	0.04	0.18
	$\bar{w}$	1.50	41.64	12.08	42.61	0.04	2.13

TABLE 4

Mean Mineralogical Composition of Flows

Excluding Vesicles

Flow		%Plag.	%Ol	%Gl+Au +Mag	%Idd	%Fe-min.
San Miguel	$1\bar{n}$	40.56	14.10	43.54	1.13	0.67
	$\bar{w}$	39.79	12.75	41.27	1.74	4.52
Santo Tomas	$1\bar{n}$	33.99	9.52	56.23	0.00	0.26
	$\bar{w}$	33.17	9.26	53.21	0.00	4.37
Santo Tomas	$2\bar{n}$	33.31	10.33	56.13	0.05	0.16
	$\bar{w}$	33.18	9.79	53.79	0.10	3.15
Santo Tomas	$3\bar{n}$	32.85	11.94	54.88	0.12	0.18
	$\bar{w}$	30.86	11.18	54.60	0.68	2.69
Black Mountain	$6\bar{n}$	42.20	12.50	45.04	0.05	0.21
	$\bar{w}$	42.27	12.26	42.26	0.04	2.16

see Appendix A).

A histogram representing the relative variation of WI_{Fe} between nonweathered (n) and weathered (w) portions of the five analyzed flows is shown in figures 2 and 3. There exists a distinct separation for WI_{Fe} that increases with increasing age of the flows; the San Miguel flow being the oldest, the three Santo Tomas -1, -2, and -3 flows following and the Black Mountain -6 being the youngest. The difference $\Delta(WI_{Fe})$, between the weathered and nonweathered parts increases with age. The following $\Delta\ WI_{Fe}$ values for the five studied flows were obtained from:

$$\Delta\ WI_{Fe} = \overline{WI}_{Fe(w)} - \overline{WI}_{Fe(n)}$$

were: $\overline{WI_{Fe}(w)}$ is the average weathered WI_{Fe}, and
$\overline{WI_{Fe}(n)}$ is the average nonweathered WI_{Fe}

San Miguel	:	6.96
Santo Tomas-1	:	6.62
Santo Tomas-2	:	4.70
Santo Tomas-3	:	3.84
Black Mountain-6	:	3.52

These values were plotted against the flow age in Figure 4.

Thickness of weathered layer

The thickness of the weathered surface was measured at several parts of every thin-sections containing a weathered sample, and then averaged. The average thickness of all the weathered samples of each flow are as follows:

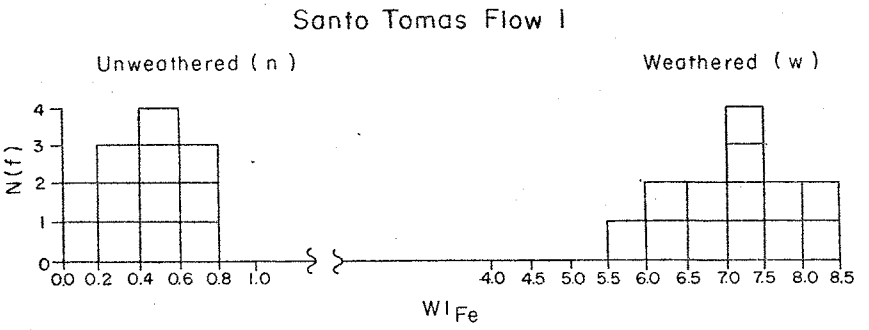

A.

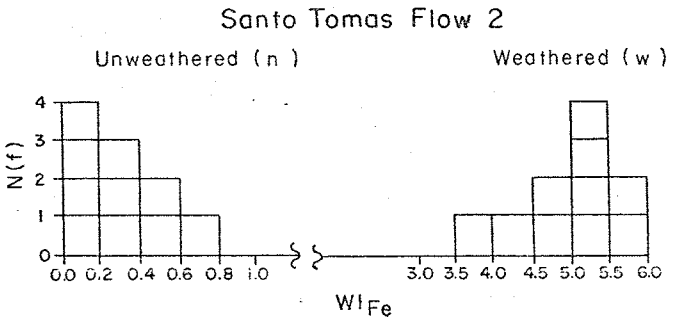

B.

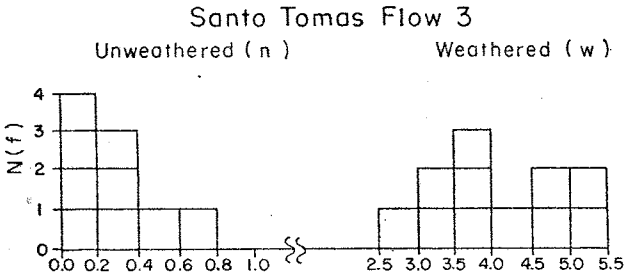

C.

$$WI_{Fe} = \frac{100 \times (\text{Fe-mineral})}{100 - (\text{Plag} + \text{Vs} + \text{Fe-mineral})}$$

FIGURE 2

Histogram of WI_{Fe} for the Santo Tomas Flows

San Miguel

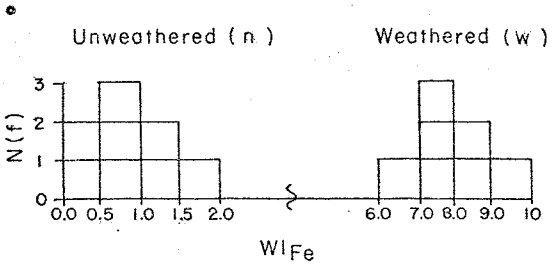

A.

Black Mountain Flow 6

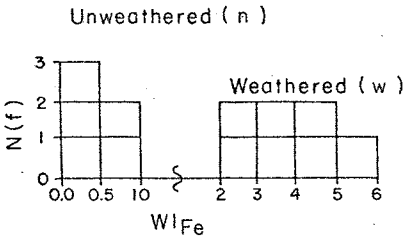

B.

$$WI_{Fe} = \frac{100 \times (\text{Fe-mineral})}{100-(\text{Plag}+\text{Vs}+\text{Fe-mineral})}$$

FIGURE 3

Histogram of WI_{Fe} for the San Miguel and Black Mountain–6 flows

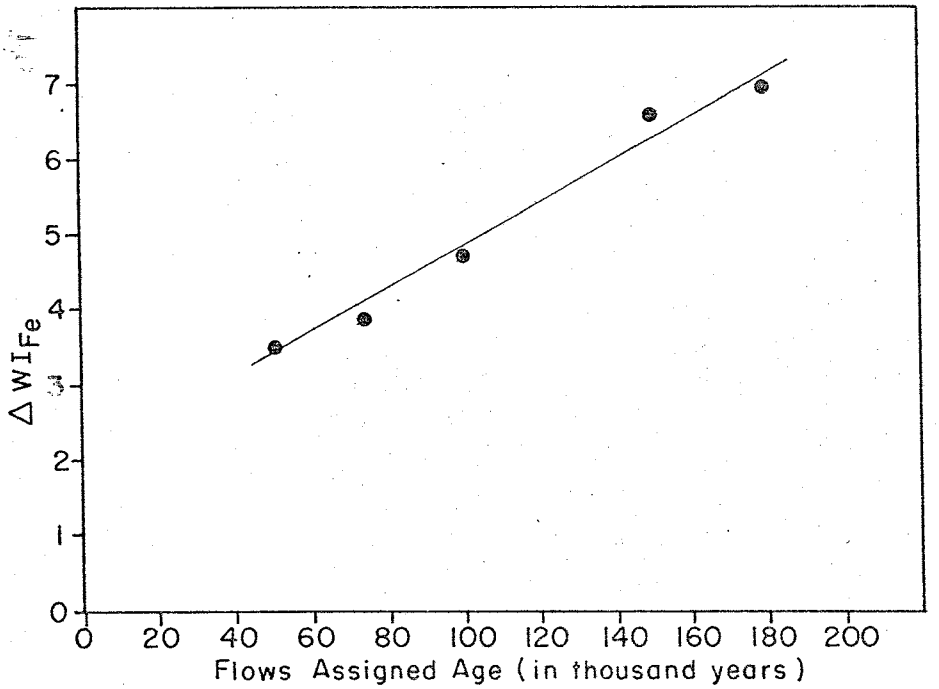

FIGURE 4

Effect of Weathering on ΔWI_{Fe}

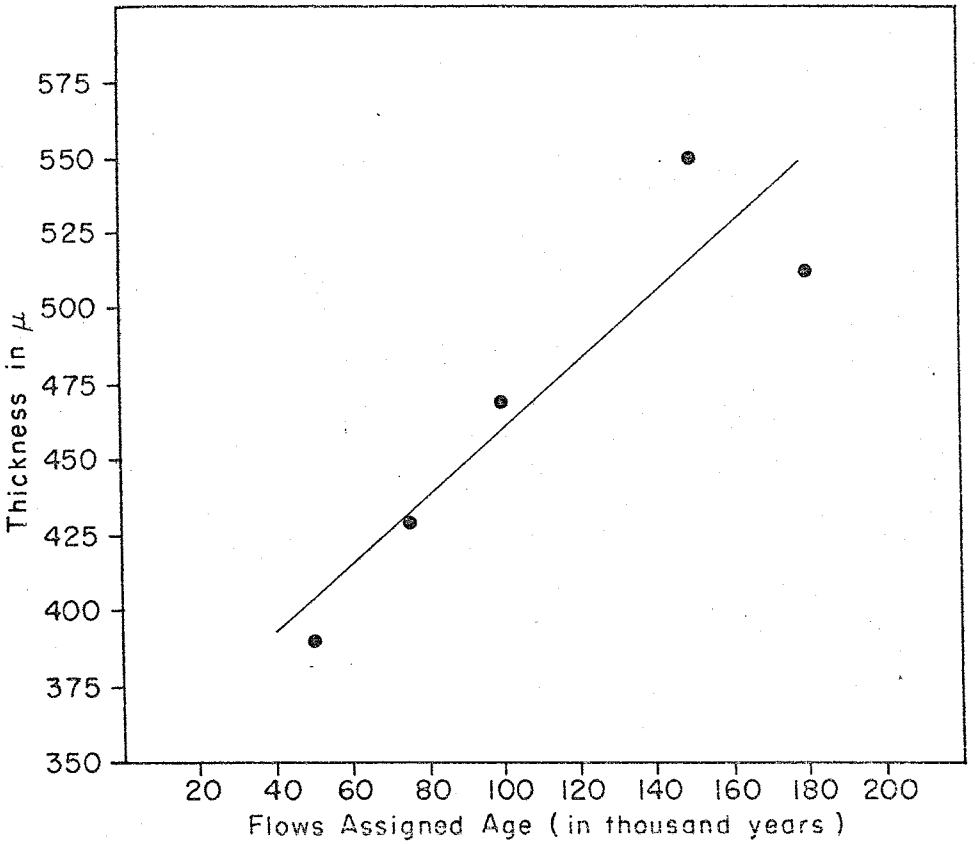

FIGURE 5

Altered-Layer Thickness

San Miguel	:	512.5μ
Santo Tomas-1	:	553.5μ
Santo Tomas-2	:	471.5μ
Santo Tomas-3	:	430.5μ
Black Mountain-6	:	389.5μ

The thickness is plotted versus the flows assigned ages in Figure 5.

Chemical Observations

Sample preparation of rocks containing weathered materi al is subject to error by loss of fine material which is not part of the soil nor wind supplied detritus. It causes an error in the chemical analysis of what is termed weathered. This error is not measurable.

Rock samples when referred to as weathered (w) in this section of the dissertation are defined as the result of the following preparation: rock slices resulting from preparation of weathered thin sections were crushed to smaller fragments ($<$ 5 mesh) and hand picked to contain as much weathered material as possible (color indication), but to be free from vesicle fillings.

Chemical analyses of briquettes prepared as described in appendix A were analyzed chemically using the x-ray fluorescent technique. The samples were analyzed for the following elements: silica, alumina, iron, calcium, titanium, magnesium, sodium, potassium and phosphate and three trace elements: nickel, cobalt and chromium. The results are represented in Table 17 Appendix B. Most analyses total to less than 100% because the samples were not analyzed for manganese and water, and because the total amount of iron was expressed as FeO. The high coefficient of variation (4.14%) of the alumina analyses

(Table 13 Appendix A) might be the cause for a few analyses to exceed 100%. Table 5 summarizes the average gains and losses of every analyzed element as a result of the natural weathering process.

In the older flows the calcium content increases as a function of age due to the formation of caliche. In humid climates calcium depletion during weathering is very noticeable (Craig and Laughman, 1964; McLaughlin, 1955). In an arid environment the ions leached from the rock are not completely removed because of high evaporation, but stay on the surface or in vesicles and cracks. The water contains carbon dioxide from the air and with the calcium forms calcium carbonate. Other ions with the appropriate size and charge might substitute for Ca^{++} in the lattice. In the experimental weathering section of the dissertation this phenomenon will be discussed further.

In the younger flows potassium is leached consistantly, but in the San Miguel flow there is relatively less depletion than in the younger basalts. This may be a spurius result due to the small number of samples analyzed for this flow, or rather because small amounts of amorphous clay (kaolinite?) on the surface of this flow. This might support Helgeson's idea (1971) that small amounts of amorphous clays form as a result of chemical weathering of minerals in a relatively short time. The decrease in the relative amount of silica leached with time might suggest that some of the silica forms clays that absorb some of the leached potassium.

TABLE 5

Average Chemical Changes between Weathered and Nonweathered Portion of the Flows.

(Deviation in terms of weathered minus non weathered)

	San Miguel	Santo Tomas-1	Santo Tomas-2	Santo Tomas-3	Black Mountain-6
$\%SiO_2$	- 0.56	- 0.77	- 1.21	- 1.35	- 1.39
$\%Al_2O_3$	- 1.41	- 0.37	- 0.76	- 1.04	- 0.35
%FeO	+ 1.01	+ 0.85	+ 0.78*	+ 0.56	+ 0.39
%CaO	+ 1.21	+ 0.39	+ 0.17	+ 0.05	- 0.22
$\%TiO_2$	+ 0.24	+ 0.17	+ 0.16	+ 0.14	- 0.20
%MgO	+ 0.85	+ 0.65	+ 0.89	+ 1.03	+ 0.33
$\%Na_2O$	- 0.77	- 0.65	- 0.56	- 0.58	- 0.45
$\%K_2O$	- 0.14	- 0.28	- 0.23	- 0.21	- 0.22
$\%P_2O_5$	- 0.03	+ 0.04	+ 0.04	+ 0.03	+ 0.14
NiO (ppm)	+15.00	+180.00	- 9.00	+19.00	+72.00
CoO (ppm)	+53.21	+ 10.81	+23.14	+22.46	+13.90
Cr_2O_3 (ppm)	+ 7.38	+ 6.82	+ 2.80	+ 2.63	+ 3.57

*Excluding sample 2-8n.

Variation in iron valence

Iron is present in basalts in two different chemical species: Fe^{+2} and Fe^{+3}. X-ray fluorescent analysis can report only the total iron content expressed as one of the oxides, in this study FeO. As a result of weathering iron undergoes two major changes: (a) iron concentration (b) oxidation of the ferrous ion to ferric ion. Several samples of weathered and nonweathered portions of Santo Tomas -1, -2, -3, and one pair of samples from the Black Mountain -6 were analyzed, for Fe^{+2} and Fe^{+3} by the method described in Appendix A. The results are listed in Table 6 and shown in Figure 7. The change in this ratio during weathering is expressed as $\Delta(Fe^{+2}/Fe^{+3})$ and is given by:

$$\Delta(Fe^{+2}/Fe^{+3}) = (Fe^{+2}/Fe^{+3})\,n - (Fe^{+2}/Fe^{+3})w$$

During weathering the total iron concentration (ΣFe) increased. The change in the total iron concentration is given by:

$$\Delta \Sigma Fe = \Sigma Few - \Sigma Fen$$

The flows mean change in total iron concentration $\overline{\Delta \Sigma Fe}$ is plotted versus the assigned flows age in Figure 7. Thus, iron can be used as a weathering index both as total iron and as valence ratio.

Indices of weathering

Many investigators have made efforts to express the degree of weathering of rocks in simple terms. The purpose of most of these indices was to compare soils to their original rock and they were

TABLE 6

Iron Weathering Indicies.

Santo Tomas - 1

Sample	Fe^{+2}	Fe^{+3}	$\leq Fe$	ΔFe	Fe^{+2}/Fe^{+3}	$\Delta Fe^{+2}/Fe^{+3}$
10- 1n	5.01	1.67	6.68	0.43	3.00	0.65
10- 2w	4.99	2.12	7.11		2.35	
6- 1n	4.88	1.83	6.71	0.65	2.67	0.86
6- 2w	4.74	2.62	7.36		1.81	
1-30n	5.71	1.91	7.02	0.53	2.67	0.82
1-17w	4.90	2.65	7.55		1.85	
1- 8n	4.94	1.78	6.72	0.54	2.78	0.80
1- 3w	4.82	2.44	7.26		1.98	
Mean				0.54		0.78

Santo Tomas - 2

2-21n	5.03	1.83	6.86	0.14	2.75	0.38
2-28w	4.92	2.08	7.00		2.37	
5- 1n	5.42	2.09	7.51	0.34	2.59	0.40
5- 2w	5.39	2.46	7.85		2.19	
4- 1n	5.39	1.83	7.22	0.18	2.94	0.34
4- 2w	5.35	2.05	7.40		2.60	
5- 3n	5.05	2.63	7.68	0.23	1.92	0.25
5- 4w	4.95	2.96	7.91		1.67	
Mean				0.18		0.34

Santo Tomas - 3

Sample	Fe^{+2}	Fe^{+3}	ΣFe	$\Delta \Sigma Fe$	Fe^{+2}/Fe^{+3}	$\Delta Fe^{+2}/Fe^{+3}$
8- 1n	5.16	2.53	7.69	0.09	2.04	0.20
8- 2w	5.04	2.74	7.78		1.84	
9- 1n	4.97	2.09	7.06	0.13	2.38	0.37
9- 2w	4.80	2.39	7.19		2.01	
Mean				0.11		0.28

Black Mountain - 6

8n	4.38	2.80	7.18	1.06	1.56	0.04
	4.37	2.87	7.24		1.52	

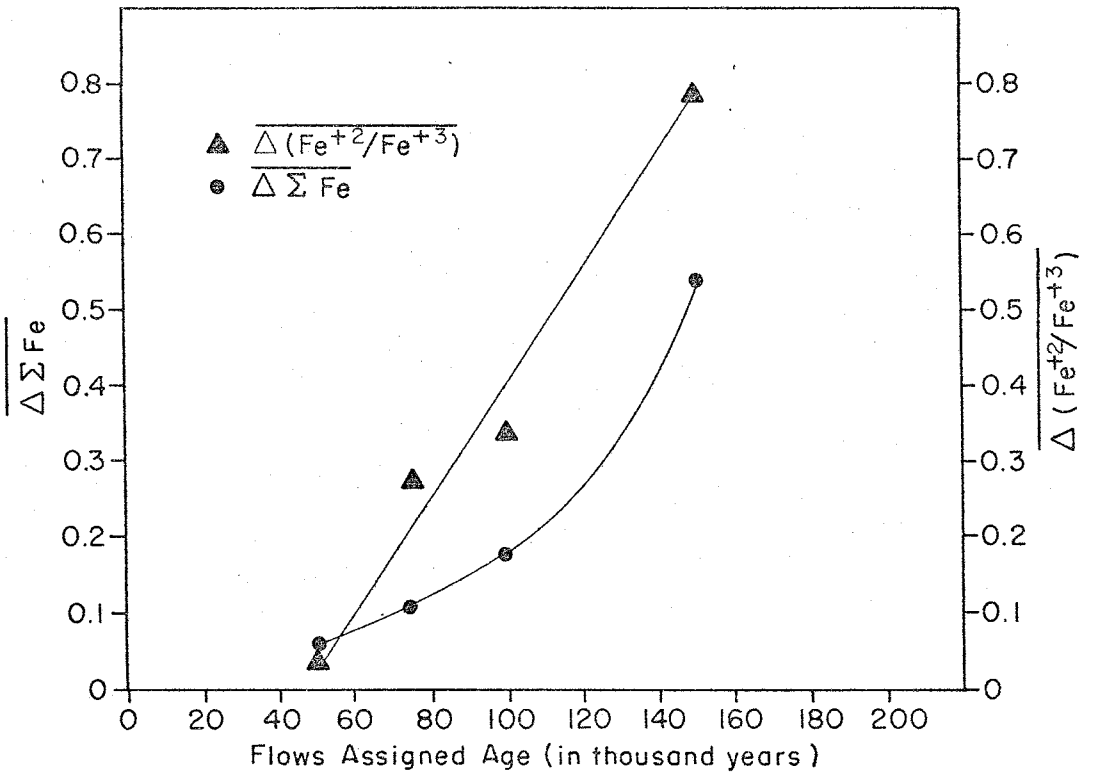

FIGURE 6

Change in Iron with Weathering Time

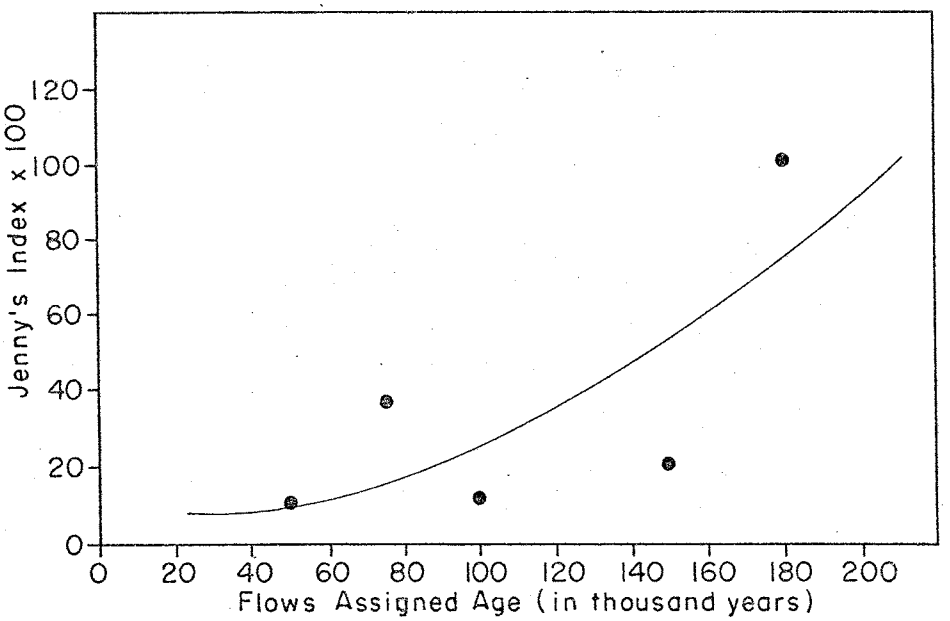

FIGURE 7
Jenny's Weathering Index

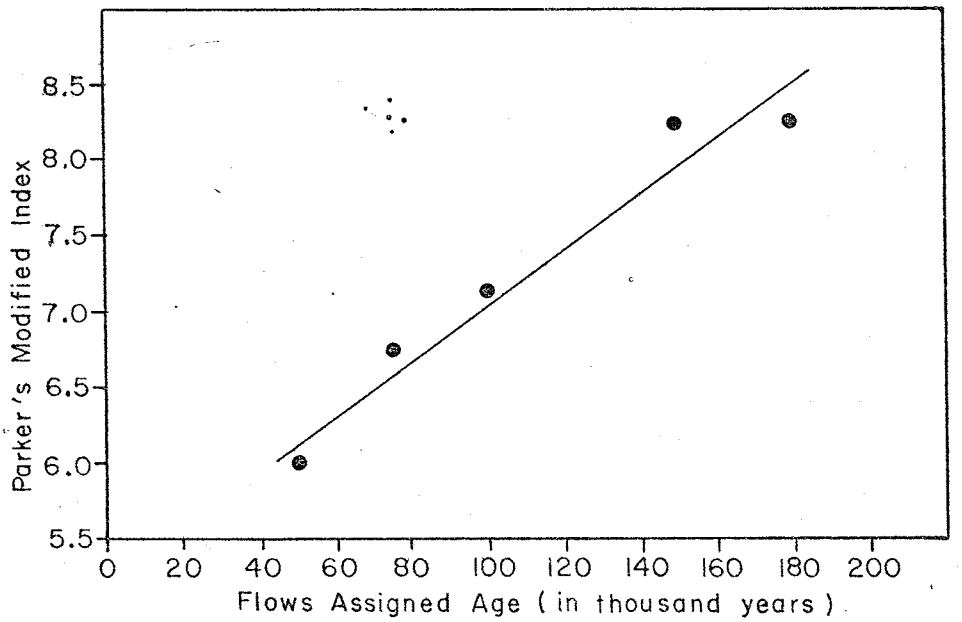

FIGURE 8
Parker's Modified Weathering Index

applied mainly to rocks in humid regions (Jenny (1931), Reich (1943), Robinson (1949), Fields and Swindale (1954), Hay (1960), Ruxton (1968), and Parker (1970)).

Excluding the Santo Tomas -3 flow Jenny's index increases non-linearly with the flow's age (Figure 8). Parker's (1970) index was unsuitable since calcium and magnesium are not depleted from these flows in this environment, hence this index was modified by using only the sodium and potassium values. Parker's modified index became:

$$\left[\frac{(Na^{+})a}{35} + \frac{(K^{+})a}{25}\right] x\ 100$$

where a indicates the atomic proportion of element defined as atomic percentage divided by atomic weight, and 35 and 25 are Nicholls (1963) values of the strength of sodium and potassium to oxygen bond. Parker's index of weathering values for these flows are plotted against weathering time in Figure 8.

The weathering indicies most suitable for measuring the degree of weathering of basalts in dry environments are:

WI_{Fe},

$\Delta \xi Fe$,

$\Delta\ (Fe^{+2}/Fe^{+3})$

Parker's weathering index and

Jenny's weathering index.

Summary and Conclusions

Mineralogical observations

Of all the basalt constituents, glass weathers faster and to a greater extent. The phase which increases in volume most is the new phase: Fe-mineral. WI_{Fe} is a weathering index clearly related to time.

Chemical observations

The most significant difference between the weathering of basalts in arid and humid climates is the concentration of calcium, magnesium and iron on the weathered surface in dry regions, while in moist regions these ions are removed from the rock. In dry environments calcium and magnesium form carbonates and the iron becomes oxidized and hydrated to form goethite. The caliche accumulations and the significant decrease of Fe^{+2}/Fe^{+3} values with weathering time indicate that carbonation and oxidation are very important weathering reactions in an arid environment.

Weathering indicies

Several indicies appear useful. A test of this would be to compute the ages of one sample as though it were an unknown. Santo Tomas-1 is used for that, and the ages as calculated from the slopes of the indicies curves are as follows:

Using	ΔWI_{Fe}	Santo Tomas-1 is	160	thousand	years
"	$\Delta \Sigma Fe$	"	" 158	"	"
	$\Delta (Fe^{+2}/Fe^{+3})$	"	" 152	"	"
	Parker's index	"	" 164	"	"

The calculated ages are not more than 14 thousand years the assigned age, and the precision is better than that of the radiometric age dating (Table 2).

EXPERIMENTAL WEATHERING

Introduction

Experimental weathering of a basalt, a glass of basaltic composition and the major basalt forming minerals have been conducted. Four types of experiments were carried out and the chemical and mineralogical changes were monitored both in the rock and in the solution. Distilled water (electrical conductivity = 1.0×10^{-6} - 1.2×10^{-6} Ω^{-1} - cm^{-1}) was the solution used during the whole investigation.

Sample Preparation

Basalt

The basalt used in all the experiments was a fresh sample from Carrizozo, New Mexico (Car 9). This sample served as a standard in the x-ray fluorescence analyses of the natural study and its chemical composition is given in Table 11 Appendix A). The sample was crushed to grains 3.5-5 mesh size, hand picked to eliminate vesicle fillings, then ground in an automatic mortar under acetone and sized into five sizes (3.5-5 mesh, 42-48 mesh, 80-100 mesh, 200-250 mesh and 270-400 mesh). The grains were cleaned from dust and smaller particles by washing with acetone. The portion used in the wetting and drying experiment was washed once with distilled water also. Chemical analysis of each sized sample indicates that the grinding and sizing had no consistant effect on the chemical composition of the rock.

Glass and minerals

The chemical analysis of the glass and the minerals used in this study are given in Table 7 . The minerals are from other localities and not separated from New Mexico basalts. The preparation is similar to that for basalt with the following exceptions:

The glass sample was prepared by completely melting fresh basalt grains (3.5-5 mesh) from the McCarthys basalts (Mac-4) in a porcelain boat and then quickly quenched in cold distilled water. The glass sample was sized to 200-250 mesh and 270-400 mesh.

Samples of labradorite and andesine were ground to 80-100 mesh, and iron mineral impurities were removed by magnetic separation. The final size used was 270-400 mesh.

The magnetite sample was separated by magnetic separation from a rock rich in this mineral. X-ray diffraction indicates the presence of some goethite and hematite. The final size used in these experiments was 270-400 mesh.

The olivine and augite used in this study were of gem quality and the final size used was 270-400 mesh.

Column Leaching Experiments

Two lucite columns 22 cm in length and 1 cm in inside diameter were used in these experiments. They were closed in the bottom by cotton. The columns were bottom fed through tygon tubing from a distilled water reservoir placed four feet above the columns.

TABLE 7

Chemical Composition[&] of Minerals and Glass
Used in Experimental Weathering

Sample	SiO_2	Al_2O_3	CaO	Na_2O	K_2O	Fe_2O_3	FeO	MgO	TiO_2	Total
Labradorite	54.59	28.11	11.47	5.13	0.60	0.49*	----	0.03	----	100.42
Andesine	62.20	12.70	2.20	9.36	5.01	0.03*	----	0.63	----	92.13
Olivine	38.60	0.27	0.09	0.09	0.02	6.82*	----	52.60	0.27	98.76
Augite	45.50	6.55	5.20	0.53	0.03	6.55*	----	29.08	0.83	94.27
Magnetite	----	----	----	----	----	86.30	14.37	----	----	100.67
Glass (Mac 4)	50.6	18.8	11.54	3.09	1.18	4.44*	----	7.82	2.49	99.98

& Wet chemical analysis.

* Total iron expressed as Fe_2O_3.

One column contained 10 g of basalt (270-400 mesh) and was leached in an average flow rate of 135 ml/day. The second column contained 10 g glass of the same size, and the average flow rate was 65 ml/day. In the beginning of the experiment the flow rate was mechanically controlled in both columns, but later as the rock and glass fragments consolidated the mechanical control device had to be removed and the flow rate was self controlled. The flow rate decreases gradually with time, and the values given are the average of the flow rate during seven months.

Three months after the beginning of the experiment light brown specks resembling the naturally occurring Fe-mineral appeared in the column containing the glass. The small grains were located in the little tunnels the water formed as it worked its way up the column, and also close to the top of the column. The grains inside the tube grew and became darker in color with time (Plates A and B).

A Column Evaporating Experiment

A column of the same kind and size as used in the column leaching experiments was used in this investigation. Ten grams of glass (270-400 mesh) were placed in the column which was filled with distilled water to the top of the glass surface and allowed to evaporate at room temperature. An amount of water equivalent to that evaporated was manually added to the top of the glass every forty-eight hours. The

experiment was carried on for four months. Small brown specks identical to those described in the column leaching experiment developed in the glass, and on the sample surface a thin white film appeared. The white top was removed from the column and examined optically and by x-ray diffraction. The x-ray diffraction analysis did not show any diffraction peaks but the optical observations revealed the presence of a crystalline phase which had a radiating fibrous habit, showed under crossed nicols a pseudo-uniaxial figure and had high birofringence. No other optical properties could be determined because the mineral was very fine grained and in small amount. The mineral was soluble in dilute hydrochloric acid with effervesence. From the observed properties it appears that this mineral is aragonite. The brown opaque phase could not be identified optically or by x-ray diffraction.

Short Term Leaching Experiments

In these experiments a basalt, a glass and the minerals: labradorite, olivine, augite and magnetite were each stirred in distilled water. The conductivity of the contact solution was measured in intervals of a few minutes or hours. Since the conductivity is a function of the concentration of ions present in solution, it indicates the relative solubility. From total dissolved solid analysis and conductivity measurements using linear regression analysis the following relationship for basalt dissolution in distilled water at 25°C has been obtained:

$$\text{T. D. S. (ppm)} = 0.65 \text{ E. C. } (10^{-6}\ \Omega^{-1} - \text{cm}^{-1}) + 8$$

When the change in the conductivity was no longer noticeable the water was changed. Every change in water initiated a new run with beginning time considered as the final time of the previous run.

Basalt experiments are reported as a representative example of all the solids since behavior of minerals and glass is similar to that of basalt with the exception of final fluid concentrations.

Basalt experiments

In these experiments three grain sizes of the basalt Car-9 were used 3.5-5 mesh, 200-250 mesh and 270-400 mesh. The conductivity of the first four runs of grain size 200-250 mesh is plotted versus time in Figure 10: all the runs of all the grain sizes behave in the same manner. The curves were plotted by many measurement points. For the sake of clarification the points are shown only for one curve. Regardless of grain size most of the soluble material is leached out in the first 30 minutes.

The rate of solution is greater with the increase in surface area for all runs. Run number three for all sizes was continued for 170 hours and the conductivity of the different grain sizes is shown in Figure 11. The conductivity at the earliest time of stable conductivity for each run is plotted versus time of that conductivity in Figure 12. The number of every specific run for each grain size is indicated on the plots. This figure indicates that more time is needed to reach stability of fluid concentration with total time of water-solid contact. This means the rate of release of ions to the liquid decreases with total time of liquid-

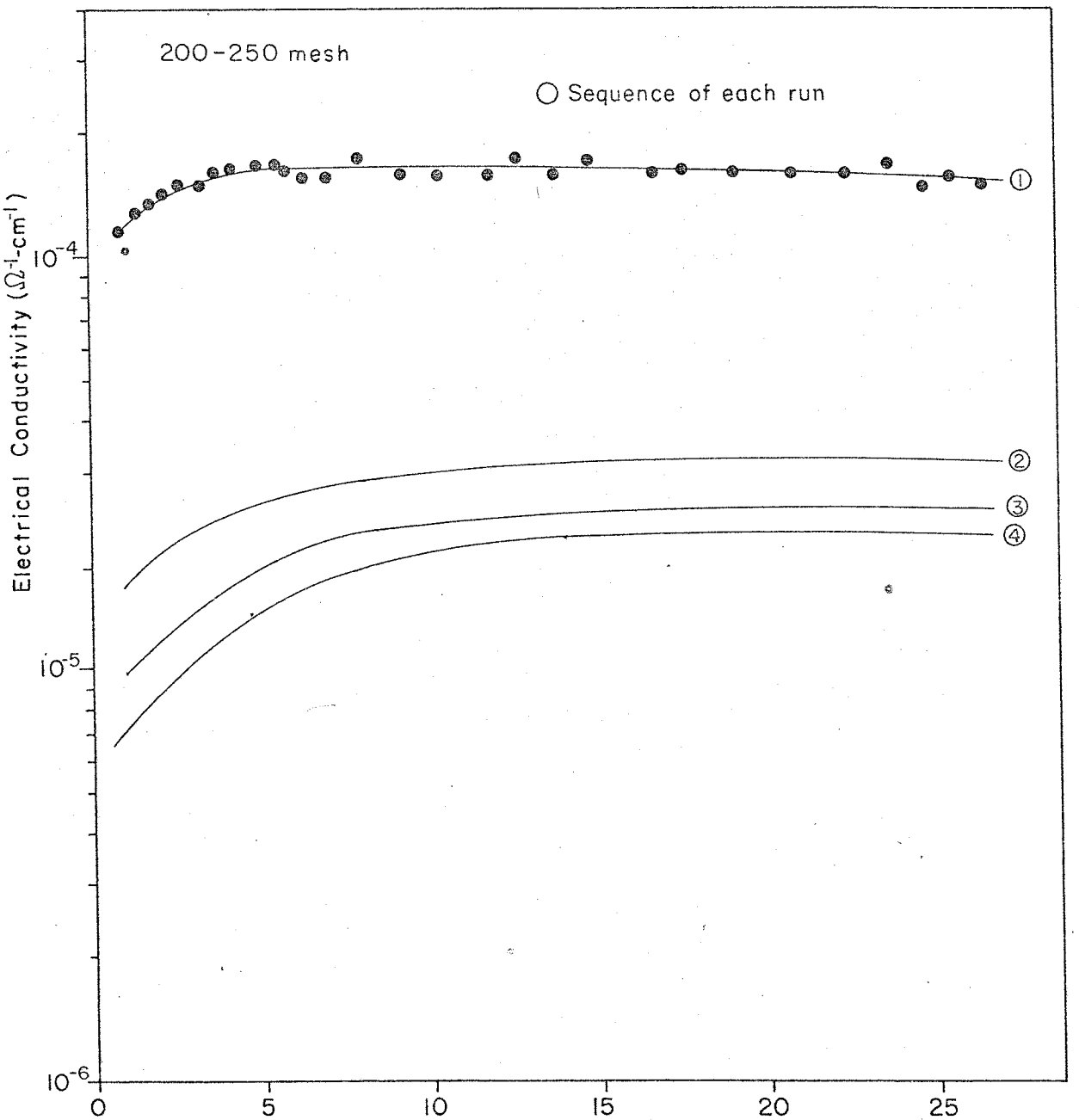

FIGURE 9
Basalt Weathering Solution

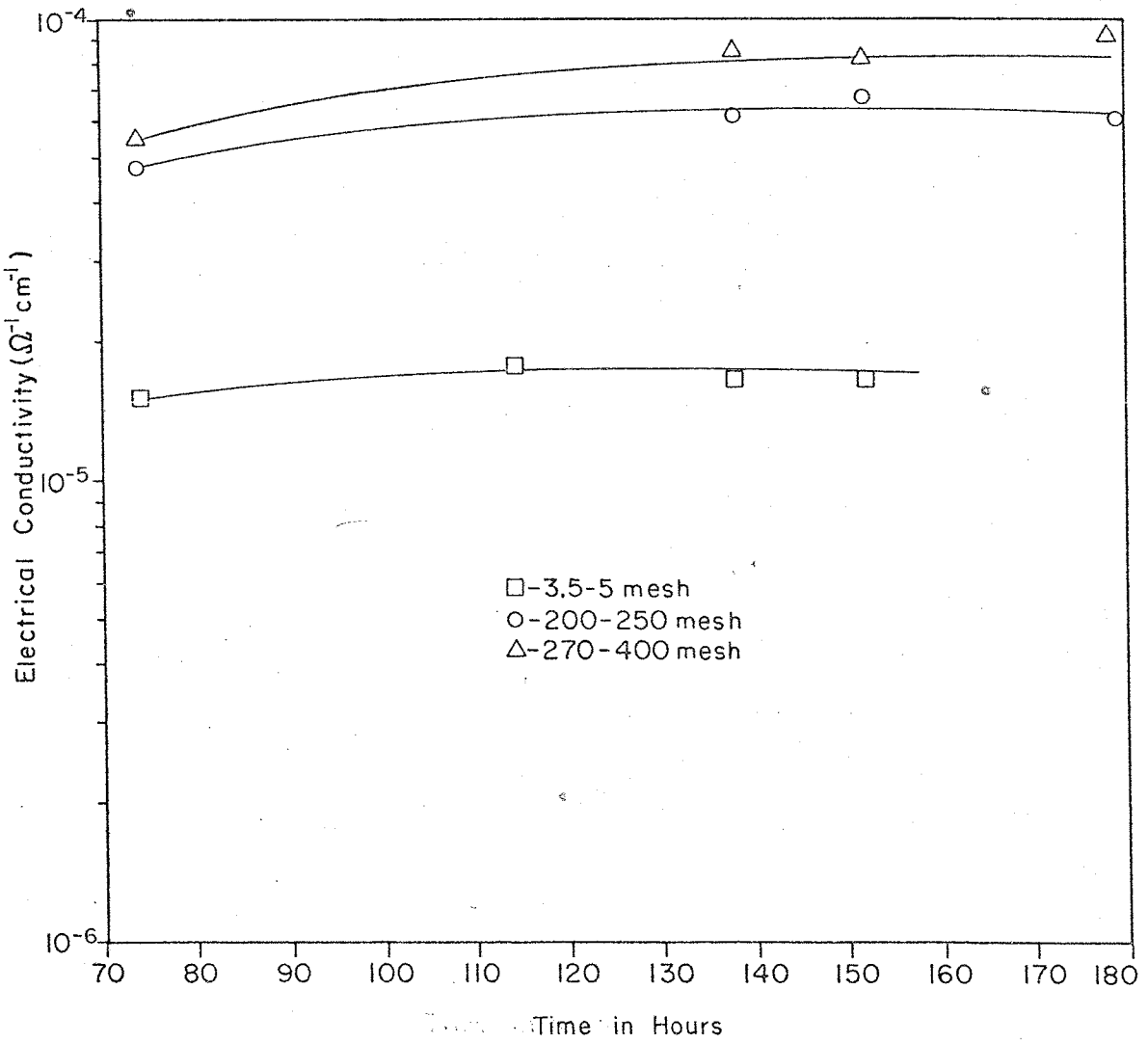

FIGURE 10

Grain Size Effect on Basalt Weathering Solution

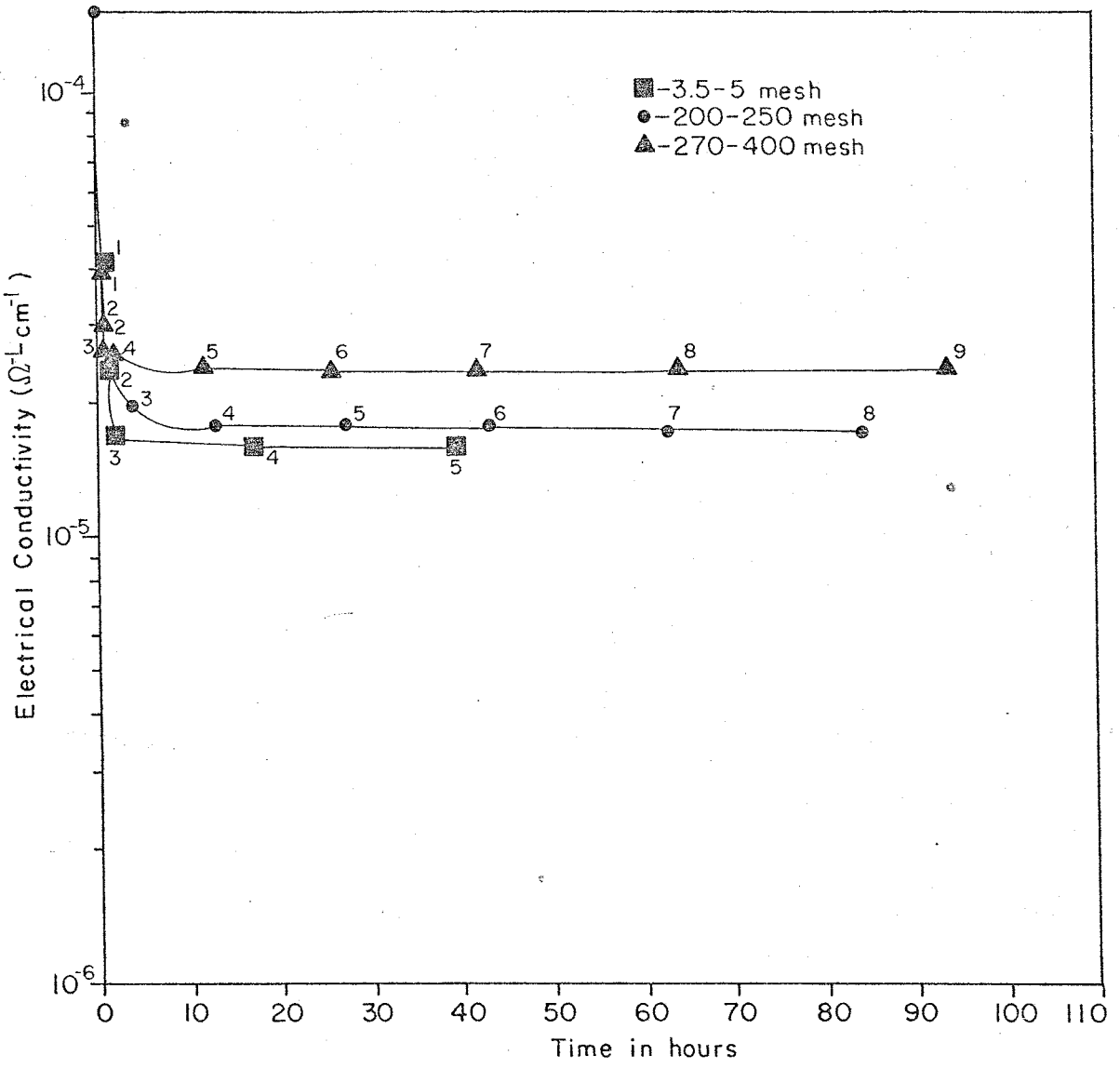

FIGURE II

Rate of Attainment of Stable Conductivity

solide contact.

Glass experiments

Two short term experiments with glass were conducted. In the first, one gram of glass (Mac-4) was added to 100 ml of distilled water and in the second, 10 g of this glass were placed in 100 ml of water. The conductivities of the two solutions do not reach the same values not even after ten runs. The solubility is a function of the $\frac{\text{weight solid}}{\text{volume solution}}$ ratio. Burkett (1970) in his work with basaltic glasses observed the same phenomenum. Because the conductivity (solubility) is a function of this ratio, the reaction is not controlled by thermodynamic equillibrium.

At the end of each run the solutions were analyzed for silica, alumina, sodium, potassium, calcium, magnesium, iron, bicarbonate and pH. The results are listed in Table 18 Appendix B. From the chemical composition of the glass solutions the following stable phases may be present at 25°C: In the system H_2O-Al_2O_3-CO_2 - MgO-SiO_2 (Helgeson et al, 1969, pg 23) the solution shows stability in the gibbsite field, in the system H_2O-CO_2-FeO-MgO the stable phase is siderite unsaturated with respect to FeO, (Helgeson et al, 1969, pg 185), in the system H_2O-Al_2O_3-CaO-CO_2 - Na_2O-SiO_2 the stable phase is leonhardite (Helgeson et al, 1969, pg 109) and in the system H_2O-Al_2O_3-MgO-SiO_2 Mg-montmonillonite may form (Helgeson et al, 1969, pg 144).

To determine the most probable phase to form from all the possibilities the free energies for the suitable reactions should be

calculated. For the reaction: Leonhardite ⟶ Mg-montmorillonite

$$\underset{\text{Leonhardite}}{7Ca_2Al_4Si_8O_{24}\cdot 7H_2O} + 2Mg^{+2} + 24H^{+} \downarrow$$

$$12Mg_{1/6}Al_{7/3}Si_{11/3}O_{10}(OH)_2 + 14Ca^{+2} + 12H_4SiO_4 + 25H_2O$$

Using the following formula:

$$\Delta G_{Reaction} = \Delta G^{o}_{products} - \Delta G^{o}_{reactants} + RT \ln \frac{a(Ca^{+2})^{14}a(H_4SiO_4)^{12}}{a(Mg^{+2})^{2}a(H^{+})^{24}}$$

Substituting the free energies of formations and the proper activities yields: ($\Delta G_{Reaction} > 0$) which indicates that this reaction does not occur spontaneously, and the probability of forming leonhardite is higher than that of Mg-montmorillonite.

For the reaction: leonhardite ⟶ gibbsite:

$$\underset{\text{leonhardite}}{Ca_2Al_4Si_8O_{24}\cdot 7H_2O} + 4H^{+} + 13H_2O \downarrow$$

$$\underset{\text{Gibbsite}}{4Al(OH)_3} + 8H_4SiO_4 + 2Ca^{+2}$$

the free energy for this reaction is negative (ΔG reaction < 0), indicating that gibbsite is the most stable phase under the experimental conditions.

Mg-montmorillonite ⟶ leonhardite ⟶ gibbsite

Since siderite has no ions in common with the other possible phases it is impossible to treat it in the same manner and thus, under the experimental conditions glass may form gibbsite and siderite (or any

other, more stable iron species).

Mineral experiments

The final conductivities of mineral solutions are given in Table 8 . The final solutions were analyzed for major elements and are reported in Table 18 Appendix B.

The chemical composition of the labradorite solution indicates that in the system: H_2O-Al_2O_3-CaO-CO_2-Na_2-SiO_2 (Helgeson et al, 1969, pg. 103) kaolinite is the most stable phase. The composition of the olivine solutions suggests the formation of gibbsite in the system: H_2O-Al_2O_3-CO_2-MgO-SiO_2 (Helgeson et al, 1969, pg. 23), and magnesite in the system: H_2O-CO_2-FeO-MgO (Helgeson et al, 1969, pg. 185).

The composition of the augite solution indicates the stability of gibbsite in the system: H_2O-Al_2O_3-CO_2-MgO-SiO_2 (Helgeson et al, 1969, pg. 23), and kaolinite in the system: H_2O-Al_2O_3-CaO-Na_2O-SiO_2 (Helgeson et al, 1969, pg. 109). Since ΔG for the reaction:

$$\underset{\text{kaolinite}}{Al_2Si_2O_5(OH)_4} + 5H_2O \longrightarrow 2\underset{\text{gibbsite}}{Al(OH)_2} + 2H_4SiO_4$$

is negative, gibbsite probably forms as the result of augite weathering under the experimental conditions.

From the results of these experiments, considering the ratio $\frac{\text{weight solid}}{\text{volume solution}}$ used, it is possible to conclude that the basalt components stability in water is in the following order: labradorite > magnetite > augite > olivine > glass, which is in good agreement with Goldich's (1938)

TABLE 8

Results of Short Term Leaching of Minerals and Glass (270-400 mesh)

Mineral	$\frac{\text{weight solid}}{\text{Volume Solution}}$	Final conductivity (in $r^{-1} - cm^{-1}$)
Labradorite	10/100	2.40×10^{-6}
Olivine	3/100	1.00×10^{-5}
Augite	1/100	2.50×10^{-6}
Magnetite	3/100	2.00×10^{-6}
Glass	10/100	2.25×10^{-5}
Glass	1/100	4.50×10^{-6}

stability principle.

Long Term Leaching Experiments

Basalt experiments

Long term leaching experiments were carried out in order to establish the disolution mechanism after the reaction reaches stability. Four 2-gallon polyethylene bottles were filled with five liters of distilled water and continuously tumbled. Each bottle contained 15 g of four sizes of basalt Car-9 (I = 3.5-5 mesh, II = 42-48 mesh, III = 80-100 mesh and IV = 200-250 mesh). A bottle of the same kind was filled with water only served as a blank. Once a week the resistivity was measured and after several weeks the water was changed. Every change in water initiates a new run. Resistivity measurements of the water in the blank bottle showed no noticeable changes which indicated that the polyethelene bottles did not release or absorb any measurable amounts of ions and all changes in solutions were due to reactions between the rock and the water only.

The behavior of the solution conductivity changes with respect to time are analogous to that of the short term leaching experiments, thus the curves are not shown.

At the end of each experiment the solutions were analyzed for major and trace elements. The solutions were concentrated twenty fold using the Bio-Rad 50 W-X12 100-200 mesh hydrogen form ion exchange as described in Appendix A. The chemical composition of

TABLE 9

Analyses of Filtrate from run 6 (in ppm)

Size	SiO_2	Al_2O_3	Na	K	Ca	Mg	Fe	HCO_3^-	pH
I	1.25	0.07	0.10	0.05	0.50	0.04	0.12	2.00	7.86
II	1.43	0.09	0.10	0.05	0.50	0.04	0.12	2.00	7.82
II	1.25	0.07	0.12	0.05	0.50	0.04	0.12	2.00	7.90
IV	0.83	0.10	0.15	0.05	0.60	0.04	0.12	2.00	8.02

TABLE 10

Relative mobility* of cations from run 6.

Size	SiO_2	Al_2O_3	Na^+	K^+	Ca^{+2}	Mg^{+2}	Fe
I	0.94	0.091	2.35	2.27	3.49	0.61	0.45
II	1.03	0.112	2.25	0.00	3.33	0.59	0.43
III	0.94	0.091	2.94	0.00	3.49	0.61	0.45
IV	0.68	0.140	4.11	0.00	4.50	0.66	0.49

*Expressed as: $\frac{\text{mole \% in solution}}{\text{mole \% in rock}}$

the major element in solution of the sixth run is given in Table 9 .

Calculations based on the chemical composition of this solution (as done for the short term leaching solutions) indicates the formation of leonhardite in the system H_2O-Al_2O_3-CaO-CO_2-Na_2O-SiO_2 (Helgeson et al, 1969, pg. 117), gibbsite in the system H_2O-Al_2O_3 - CO_2-MgO-SiO_2 (Halgeson et al, 1969, pg 23), siderite (unsaturated with respect to FeO) in the system H_2O-CO_2-FeO-MgO (Helgeson et al, 1969, pg 185), and Mg-montmorillonite in the system H_2O-Al_2O_3-MgO-SiO_2. Thermodynamic data imply (as described in the previous section) that gibbsite and siderite (or any other more stable iron species) can form as a result of weathering under the experimental conditions.

The relative mobility of the cations from run 6 expressed as $\frac{\text{mole \% in solution}}{\text{mole \% in rock}}$ are given in Table 10 . The most soluble cations are calcium, the alkalis and silica in the following order: Ca > Na > K > Si > Fe > Mg > Al.

Mechanism of ion release

Similarly to the short-term leaching experiments, it appears that stability is reached shortly after the water comes in touch with the rock, but solubility definitely continues after stability has been reached, although at a lower rate. During the first thirty minutes of each run cations from the rock surface are leached into the fresh solution. Once stabilization is achieved the relatively rapid dissolution of the rock due to leaching is over and a mechanism of removing cations from the rock at a lower rate starts. This mechanism is probably diffusion.

Fick's law of diffusion expresses the change in the concentration C, of a material at a particular place in space with the coordinate X, as a function of time t. Fick's law was expressed in the form of an equation by Nernst (1911):

$$\frac{dc}{dt} = D \frac{d^2c}{dx^2}, \tag{3}$$

where D is the diffusion coefficient, which is independent of x and t. When the initial condition is: C=Co at t=o and the boundary condition is: C = 0 at x = 0 the solution of Fick's equation for the case of diffusion into a semi-infinite solid from a plane surface is (Carslaw and Yaeger, 1971, p. 58):

$$C = Co \operatorname{erfc} \frac{x}{2\sqrt{Dt}}$$

Where erfc x = 1- erfx , and

$$\operatorname{erfx} = \frac{2}{\sqrt{\pi}} \sum_{n=0}^{\infty} \frac{(-1)^n X^{2n+1}}{(2n+1)\, n!}$$

hence

$$C = Co \left[1 - \frac{2}{\sqrt{\pi}} \sum_{n=0}^{\infty} \frac{(-1)^n}{(2n+1)\, n!} \left(\frac{x}{2\sqrt{Dt}} \right) \right]$$

To a first approximation for $x < 1$, only the first term in this series is considered and the solution can be written as:

$$C = Co \left(1 - \frac{2}{\sqrt{\pi}} \cdot \frac{x}{2\sqrt{Dt}} \right)$$

or $$C = Co - \frac{Cox}{\sqrt{\pi Dt}} \Longrightarrow \frac{Co-C}{Co} = \frac{x}{\sqrt{\pi D}} \cdot \frac{1}{\sqrt{t}}$$

For a given X = Xc

$$\frac{Co - C}{Co} = Q^{-1} = \frac{Xc}{\sqrt{\pi D'}} \cdot \frac{1}{\sqrt{t'}}$$

or $$Q = \frac{\sqrt{\pi D'}}{X_c} t^{\frac{1}{2}} = Kt^{\frac{1}{2}}$$

where Q is the weight of ions total weight and K is the reaction constant that states the amount of reaction occurring at any one time. When all the terms in the series are taken into consideration the equation becomes:

$$Q = Kt^{\alpha}$$

This form of the diffusion equation has been used by Lyle (1943), Douglas and El-Shami (1967), Burkett (1970) and Burkett et al. (1970) in their studies of glass alteration. Burkett et al, (1970) classified the processes taking place into three categories according to the values.

(1) $\alpha = 1$: ideal leaching
(2) $\alpha = \frac{1}{2}$: ideal diffusion
(3) $\alpha < \frac{1}{2}$: non-ideal diffusion

By plotting ln Q versus ln t, α is the slope. For basalts of size 200-250 mesh ln Q is plotted versus ln t in Figure 13. The slopes were determined using linear regression analysis. During the first thirty minutes of each run leaching takes place (not shown in Figure 13) and later diffusion takes place as shown by the change in α with time. Similar plots of the other grain sizes follow the same pattern. The values suggest that after initially rapid leaching "stabilization" with respect to short intervals of time is reached resulting in a thin alumino-

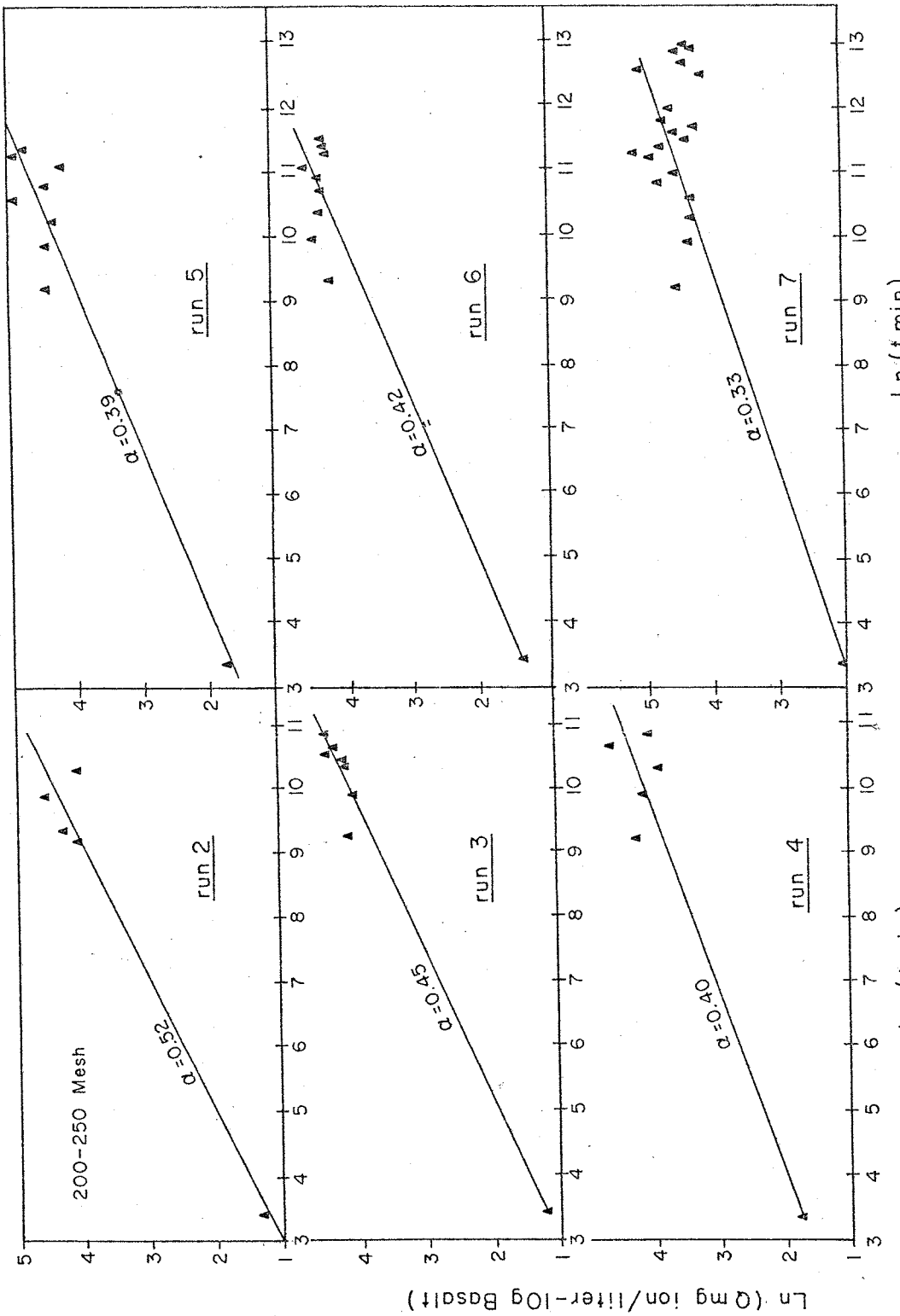

FIGURE 12
Results of Basalt Long Term Leaching Experiment

silicate layer on the surface. Such a silicate layer has been proposed and discussed by Wollast (1967), De-Vore (1958), Correns (1961) and Helgeson (1971). As weathering continues ions from below this layer diffuse through it into the solution.

Microscopic observations do not show any apparent changes in the mineralogy. X-ray diffractions of the rock powder removed at the end of the fourth, fifth, and sixth run show some broadening in some of the smaller mineral peaks and a significant decrease in their intensity.

Glass and mineral experiments

Three long leaching runs of glass were conducted similarly to the basalt experiments. The slopes obtained when plotting ln Q versus ln t were decreasing gradually with the increase in the run number. The α values are for the first run 0.41 and 0.34 for the second and third runs.

Labradorite, andesine and olivine behaved in the same manner in similar experiments.

Experiments of Alternate Wetting and Drying

The short and long term experiments have demonstrated that leaching and diffusion are taking place as rocks come in contact with water. The results of these mechanisms are significant in nature in humid regions where the precipitation is high and especially frequent. In arid environments, the amount of the precipitation is slow, and the rains are separated by long periods of dryness. In such regions leach-

ing and diffusion accompany the process of alternate wetting and drying.

During the process of alternate wetting and drying, evaporation draws the soluble ions to the surface during the drying period. When all the moisture within the rock is removed during the drying cycle the soluble ions crystallize partly on the surface and partly along pores, cavities and cleavage planes. The most effective cycle is one in which the rock is completely dried and then completely saturated in one cycle.

An apparatus which automatically wet and dried samples was constructed. The instrument is described in Appendix C. The samples used in these experiments were 270-400 mesh in size. In addition to the regular sizing and acetone cleaning the samples were washed once with distilled water to remove water soluble impurities that have been proven to be present by the dissolution experiments. The amount of water used to completely wet the samples ranges between 2.8 to 3.5 ml. cycling was continuous and consisted of 18 seconds of wetting and 7 minutes and 42 seconds of drying. After a certain period of time the samples were removed from the cycling apparatus and washed in 100 ml of distilled water for a period of 24 hours.

Experimental Results

Basalt experiments

A sample from Carrizozo (Car-9) was treated for five periods

and an accumulative time of 668 hours. The chemical analyses of the washing solutions are listed in Table 19 Appendix B and the plots of these values versus time are shown in Figure 14.

The results show that most of the removal of cations diminishes steadily after reaching a maximum in 100 to 150 hours of cycling. Despite the fact that wetting and drying causes grain fracturing that results in fresh surfaces (Hudec and Dunn, 1966) the concentrations of most cations decreased to very low values. This may suggest the formation of secondary phases from the ions released from the sample. The chemical compositions of the wash solutions indicate that in the system H_2O-Al_2O_3-CaO-CO_2-Na_2O-SiO_2 leonhardite saturated with respect to calcite is the most probable mineral to form (Helgeson et al. 1969, pg. 112), in the system H_2O-CO_2-FeO-MgO siderite may form (Helgeson et al, 1969 pg. 186) in the system H_2O-Al_2O_3-Mg-SiO_2 Mg-montmorillonite is most stable (Helgeson et al, 1969, pg. 146) and in the system H_2O-Al_2O_3-CO_2-MgO-Na_2O-SiO_2 the solution is in the stability field of Mg-chlorite (Helgeson et al, 1969, pg. 56). ΔG for the reaction

$$\underset{\text{Mg-montmorillonite}}{6\ Mg_{1/6}\ Al_{7/3}\ Si_{11/3}\ O_{10}\ (OH)_2} + 4\ Mg^{+} + 58\ H_2O \longrightarrow \underset{\text{Mg - chlorite}}{Mg_5Al_2Si_3O_{10}\ (OH)_8} + 12\ Al(OH)_3 + 19\ H_4SiO_4 + 8\ H^{+}$$

is positive (ΔG reaction $>$ O) indicating Mg-Montmorillonite to be the more stable mineral under the experimental conditions. ΔG for the reaction:

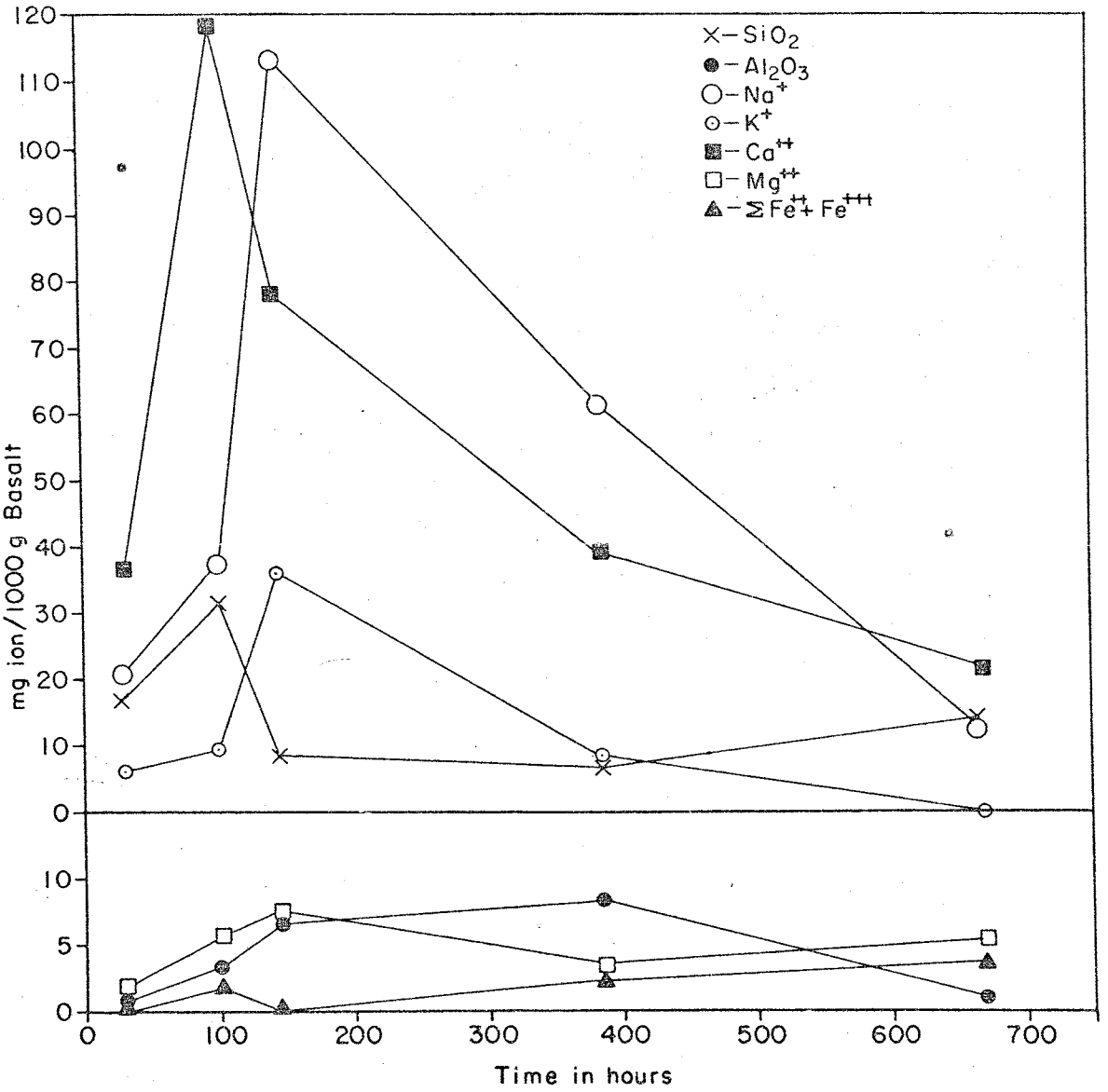

FIGURE 13

Chemical Composition of Basalt Wash Solutions
Versus Accumulative Experimental Time

$$\underset{\text{leonhardite}}{Ca_2Al_4Si_8O_{24} \cdot 7H_2O} + 2CO_2 + 15H_2O \longrightarrow 2\underset{\text{calcite}}{CaCO_3} + 4Al(OH)_3 + 8H_4SiO_4$$

is negative (Δ G reaction $<$ O), thus calcite may form in this system.

Δ G for the reaction:

$$FeCO_3 + Ca^{+2} \longrightarrow CaCO_3 + Fe^{+2}$$

is negative (Δ G reaction $<$ O) indicating that calcite is the mineral that may form under the experimental conditions.

From these data it is possible to conclude that as basalts weather in a dry environment calcite, Mg-montmorillonite and iron oxides are the most likely secondary minerals to form.

The small portion of basalt that was removed at the end of every wetting and drying period was inspected microscopically, by x-ray diffraction and by the x-ray film technique but no noticeable new phases were observed.

Glass experiments

A sample of glass Mac-4, (270-400 mesh) was treated for five periods and an accumulative time of 2045 hours. The compositions and concentrations of the washing solutions are listed in Table 19 Appendix B and the concentrations are plotted versus time in Figure 15. The results indicate that the relative amounts of ions released from the glass is higher than that removed from the basalt because the bonds

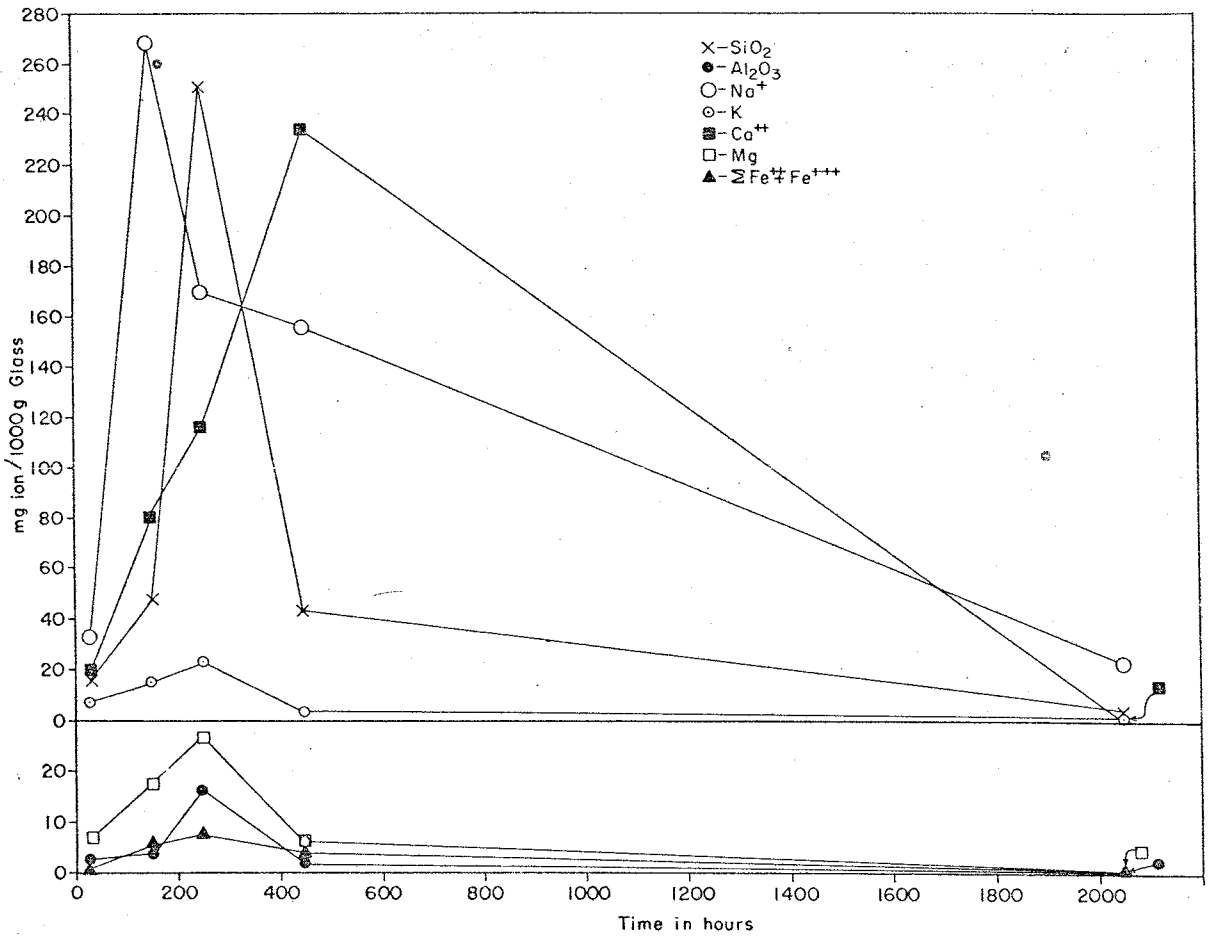

FIGURE 14

Chemical Composition of Glass Wash Solutions
Versus Accumulative Experimental Time

by which the cations are bound in the glass are less strong than in minerals. The concentrations of all cations except calcium increased in the first three periods of cycling and in the following two periods decreased sharply. Calcium was still removed during the fourth period but its concentration in the last washing solution decreased drastically. Calcium is removed faster from the basalt and to a greater extent than any other cation whereas sodium is released faster from the glass and at a higher relative concentration (Compare Figures 14 and 15).

The chemical composition of the solutions and thermodynamic considerations indicate that as glass weathers in dry environments calcite, Mg-montmorillonite and iron species are likely to form.

At the end of every period the samples were examined by optical microscope, x-ray diffraction and in some cases by x-ray powder camera and scanning electron microscope.

The glass used in these experiments was almost completely amorphous (Photomicrograph 1 and 2 Plate C). Microscopic observations after the first two periods showed very small white specks that are probably the soluble salts that have been drawn to the surface by capillary action (Photomicrograph 1 Plate D).

Two layers developed in the glass sample during the 2045 hours of wetting and drying. The upper part became consolidated into a crust that increased in thickness with time. The bottom of the sample was composed of very small reddish brown grains and became darker

(more oxidized) with time.

Calcite was identified by the x-ray powder camera technique (Table20 Appendix B), as well as by microscopic and chemical observations to be present in the crust.

Elongated fibers that appeared in the crust before the calcite formation, and were observed again after its dissolution in diluted hydrochloric acid were unidentifiable. SEM photographs of these fibers (Photomicrograph 1 and 2 Plate F) resemble attapulgite and sepiolite (Grim, 1953). These minerals are found in caliche formations in southern New Mexico. Vanden Heuven (1966) treated New Mexico caliche with a buffered solution to remove the carbonates and only then was he able to observe these vibrous clay minerals microscopically. He believed that sepiolite and attapulgite formed during the period of caliche formation and were concentrated as the carbonates were removed by high rainfall. The data of this dissertation support the suggestion of Hawley (1970) that: "much of the sepolite and attapulgite were emplaced prior to marked carbonate accumulation and that the subsequent carbonate emplacement filled in between and pushed apart the aggregates and fiberlike bodies".

Another unidentified phase was composed of some very small greenish grains rimming glass grains. The coating material looked like a gel, had a low birefringence and a lower index of refraction than the glass (< 1.6). They resemble montmorillonite (Photomicrograph 2, Plate 2) that forms in nature in similar environment (Craig and

Laughnan, 1964 and Laughnan 1969).

Simultaneous with the formation of the clay and the carbonate minerals on the crust, magnetite altered to amorphous secondary iron oxides such as geothite and hematite in the lower but oxidized portion of the sample, as indicated by the color of the bottom of these samples. This layer resembles the specks that appear on naturally weathered basalts and that were point counted in a previous part to give the weathering index WI_{Fe}.

Mineral experiments

The basalt composing minerals labradorite, andesine, augite, olivine and magnetite were treated in the same manner described for the basalt and glass samples. The chemical analysis of the wash solutions are listed in Table 19 Appendix B.

X-ray diffraction of the resulting material showed some inconsistent broadening of the smaller peaks and decrease in intensity of most peaks. The augite sample showed the development of the major calcite peak indicating the formation of calcite from this calcium rich mineral.

X-ray diffraction of the original magnetite used in this experiment shows the presence of some goethite and hematite. After the second period the goethite peaks increased in intensity and a new small goethite peak appeared (d = 1.56), the hematite peaks increased somewhat and two new peaks at d = 7.41 and d = 3.31 appeared. These peaks apparently belong to a new phase, the synthetic goethite known as β-FeOOH = Akaganeite (MacKay 1960). During the third, fourth, fifth

and sixth washing periods goethite and akaganeite peaks decreased gradually until they disappeared completely, magnetite peaks broadened and decreased in intensity while hematite peaks increased but stayed broad. These results agree with thermodynamic considerations: (Berner, 1969) that: "goethite is thermodynamically unstable relative to hematite plus water under practically all geological conditions." Thus, magnetite weathers in the following sequence: magnetite ⟶ goethite ⟶ hematite.

Summary and Conclusions

Experimental weathering in this study illustrated the following facts:

A. Short and long term experiments

During the first thirty minutes cations are leached into the water and later the dominant transfer mechanism is diffusion. The minerals peaks showed some broadening and a decrease in intensity which indicates that cation have been removed from these minerals, and the crystallographic structure has been disturbed. The cations diffuse at a low rate through a presumed alumino-silicate layer that probably forms on the surface. The rate of diffusion decreases with the increase in the number of water changes (runs).

The relative mobility of the cations in basalts is:

$$Ca > Na > K > Si > Fe > Mg > Al$$

The solubilities of the basalt and the glass are a function of weight solid/volume solution.

The relative solubility of the basalt constituents is in the following order:

glass > olivine > augite > plagioclase > magnetite

B. Evaporating and low rate leaching columns

The column evaporation glass experiment has shown that arragonite forms, on the surface of evaporation, whereas near the water path, ferric oxyhydroxide (probably goethite) is precipitated.

In the leaching column experiment, no calcium carbonate formed but an iron rich mineral grew from the glass.

C. Alternate wetting and drying experiments

The alternately wetting and drying experiments appear to be a reasonable simulation to natural weathering in arid environments. The secondary minerals that form on the glass sample are calcite and probably montmorillonite, sepiolite and attapulgite in the crust and amorphous ferric oxyhydroxide on the bottom of the sample. Calcite also forms from augite. Magnetite weathers to hematite by way of goethite, as an intermediate compound.

magnetite $\longrightarrow$ goethite $\longrightarrow$ hematite

β-goethite forms shortly after the beginning of the experiment but being less stable than α-goethite, it changes either to α-goethite or to hematite.

GEOCHEMICAL CONSIDERATIONS

Correlation Between Experimental and Natural Weathering

Weathering in moist areas

The short and long term experiments can simulate natural weathering in moist areas. The water in these tumbling experiments depletes cations from the rock as high and frequent precipitation does in nature. In high rainfall areas the water penetrates quite deep into the rock, removes the soluble weathering substances and as a result clay minerals form. These secondary minerals are rich in aluminum which is the least soluble cation. The minerals that form are mainly halloysite ($Al_2Si_2O_5(OH)_4$), hydrated halloysite ($Al_2Si_2O_5(OH)_4 \cdot 2H_2O$) or a solidified gel, allophane ($Al_2O_3 \cdot xSiO_2 \cdot mH_2O$). In the experiments conducted in this study none of these minerals were observed. Rain water and soil water however, have a higher hydrogen activity than distilled water and decompose basalts to a greater extent than the distilled water used in these experiments. The chemical analysis of the solutions suggest that over longer periods of time the experiments could result in the same secondary minerals, that form in nature over geological periods of time.

Weathering in dry areas where evaporation potentially exceeds rainfall

The alternate wetting and drying experiments and the column evaporation experiments simulate natural weathering in arid areas where

evaporation potentially exceeds rainfall. Evaporation during the drying periods draws cations from inside the rock to the surface by capillary forces. The slight wetting does not carry away the soluble weathering materials but concentrates them on the parental material. The experiments simulating weathering in semiarid to arid areas have shown the formation or potential formation of calcium carbonate, Mg-montmorillonite, sepiloite, attapulgite and ferric oxyhydroxides.

Weathering in dry areas where evaporation balances rainfall

The low rate column leaching experiment simulates weathering in areas where the rainfall and evaporation fluctuate to balance each other. The low rate leaching is sufficient to remove the soluble cations, thus the experiment resulted in no formation of carbonates. The iron removal is more complicated because it oxidizes and forms insoluble complexes. If the leaching is not done at an adequately fast rate, iron can accumulate as indicated by the results of this experiment, thus in areas where the average annual rainfall balances the evaporation in the area, no carbonates are observed on the parental rock, the clays that form vary in composition and iron hydroxides are observed (Keller, 1957).

Comparison between the natural and laboratory formation of Fe-mineral

A very small amount of reddish grains resembling the natural Fe-mineral was produced in the glass long term experiments. In the alternating wetting and drying glass experiments, these reddish grains

start developing on the bottom part of the sample, about 400 hours after the beginning of the experiment. During this time the sample undergoes 3000 cycles of wetting and drying. Assuming that in a semi-arid to arid climate, like the environment in the Black-Mountain-Santo Tomas region, there are on the average five showers per year (Reynolds, 1956), the reddish amorphous iron phase would develop in such an environment, on pure basalt glass, in about six hundred years.

It would be of interest to extend the point counting study (with the modification to point count only vesicles plagioclase, Fe-mineral and all iron bearing minerals as a whole) to younger basalts located in arid environments, and to determine the initial time of the Fe-mineral appearance.

Plagioclase Weathering

The desorption of the cations from the plagioclase lattice should proceed in the sequence Na $>$ Ca, because of the differences in their bond energies. Natural samples as well as laboratory experiments have shown albite to be by far more stable to weathering than anorthite. Marshall(1964) mentions natural anorthite complete decomposition in a time as short as 200 years.

The results of the basalt experiments of this study show that calcium has a higher relative mobility than sodium in basalts, but the glass experiments indicate that sodium has a higher relative mobility than calcium in glasses. The bond-energy influences the hydronium

replacement in the glass, but in the crystalline plagioclase the silicate structure controls the plagioclase decomposition.

There is a universal drive to increase the entropy of every system. Entropy is a quantitative physical expression of disorder. Nature prefers disorder and every ordered system is driven toward disorder by natural processes. One of the factors controlling the tendency of weathering reactants (oxygen, water, carbon dioxide, etc.) to react with parental minerals to form secondary minerals is the increase of disorder. For example, during the oxidation of magnetite to metastable maghenite (γ -Fe_2O_3) the Fe^{+2} are changed to Fe^{+3} cations and the defectiveness of the structure increases (Eitel, 1958 p. 49), and as goethite is dehydrated to hematite the entropy also increases.

Laves and Hafner (1956), (reported by Eitel, 1958) confirmed by infrared studies that the anorthite mineral (Al^{+3} : Si^{+4} = 1 : 1) is highly ordered, while the albite mineral (Al^{+3} : Si^{+4} = 1 : 3) possesses a much more disordered structure. The entropy values reported by Helgeson (1969) for albite are 50.2 cal/mole-degree and for anorthite 48.45 cal/mole degree (at 25°C). The natural process of weathering tends to break down the anorthite ordered structure to a higher degree than it disrupts the less ordered albite structure.

Caliche Formations

Caliche (calix = lime) is a term used to describe material rich in calcium carbonate (calcite) and high-silica clay minerals formed in

semiarid to arid environments. Caliche deposits are found throughout the southwestern United States, in Argentina, South Africa, Lybia, Tunis, Morocco, Algeria, Egypy, Syria, Israel, Saudia-Arabia, Spain and in Australia.

The caliche beds in southern New Mexico have been described by many authors. The most important descriptions were done by: Bretz and Horberg (1949), Ruhe (1967), Hawley and Gile (1966), Gile, Hawley and Grossman (1970), Reeves (1970, 1971). The chemical composition of these formations was studied by Aristarain (1970). Ruhe (1967) demonstrated by calculations that the country rock (rhyolite and monzonite) on which the caliche deposits he studied were located, could not be the calcium source for these formations. This conclusion need not hold true for basalts because of their greater calcium content (8-10% CaO). The possibility of calcium transportation by ground water (Reeves, 1970) is not always the answer because in many areas the water table has always been very far from the country rock. The most accepted theory that explains the caliche formation on low calcium parental rocks is that the calcium is blown into the area by winds as dust size particles in the form of calcium salts.

The five flows from the Santo Tomas-Black Mountain region, studied in this dissertation, contain caliche in cracks and very noticeable amounts are filling the basalt vesicles. Some vesicles have no openings to the surface and only water, not particles, can penetrate to the vesicles only. Such vesicles contain substantial amounts of caliche.

Although percolating water from rain would bring some soluble salts, the main source of calcium for the caliche in the vesicles seems to be the weathered basalt. It was observed that the basalt surface surrounding vesicles filled with caliche are weathered to a greater degree (contained more Fe-mineral) than empty vesicles. Vesicles that are partly filled with caliche show a greater degree of weathering on the surfaces that are in touch with the caliche.

Comparison of the chemical composition of weathered and non-weathered portions of the five examined flows in this dissertation shows that calcium and magnesium are concentrated during weathering on the weathered parts of these flows, and the concentrations of these elements increase with the increase in weathering time. Carbonates have also been formed on the surface of glass in the experiments simulating weathering in semiarid to arid climates (evaporation in room temperature and alternate wetting and drying experiments).

These facts suggest that the source of caliche in basalts is weathering.

The Origin of the Santo Tomas-Black Mountain Flows

The results of this dissertation which may help in interpreting the origin of these flows are:

(a) The weathering indicies of these flows show that the San Miguel flow is the oldest of the five examined flows. The sequence of the three Santo Tomas flows is established by the stratigraphy as well as the weathering indicies. The Black Mountain-6 flow

is the youngest of the Black Mountain flows as indicated by stratigraphy. The age dating results of the Field Research Laboratory as herein interpreted, also show that the San Miguel is the oldest of the five studied flows, the three Santo Tomas flows follow, and the Black Mountain-6 flow is the youngest.

(b) Kuno's (Kuno et al., 1957) solidification index (SI) expresses the degree of differentiation of basaltic magmas.

$$SI = \frac{100 \times MgO}{MgO + FeO + Na_2O + K_2O}$$

SI decreases with the increase in differentiation. SI values higher than 40 suggest accumulation of olivine crystals, SI values that range between 35 and 40 imply little or no differentiation and values of SI below 35 suggest differentiation of basaltic magma in the crust.

The SI values of these flows are:

San Miguel : 40.65,

The average value of the Santo Tomas flows is: 38.95,

Black Mountain-6 : 32.82,

(c) As a magma differentiates it tends to become enriched in K_2O. The average K_2O concentrations of these flows are:

San Miguel : 1.51%,

The average K_2O values of the Santo Tomas flows is: 1.56%,

Black Mountain -6 : 1.97%

These data may imply one source of crystallizing magma for all the flows in the area. The first flow to erupt was the San Miguel flow (SI = 40.65 and K_2O = 1.51). The Santo Tomas flows followed in their stratigraphic sequence; (average SI = 38.98 and average K_2O =

1.56%) and the Black Mountain-6 flow seems to be the youngest (SI = 32.82 and K_2O = 1.97).

The purpose of this investigation was to study the differences between weathered and fresh portions of these flows, thus the area had not been sampled sufficiently for an exact determination of the origin of all the flows in the Black Mountain - Santo Tomas region. More chemical data from other flows would increase the possibility of interpreting correctly the history of the whole area.

SUMMARY

The conclusions of this research which support published work are:

1. Goldich's (1938) empirical sequence of relative stability of the basalt minerals, is supported by the natural and experimental results of this study. The stability sequence is: olivine < augite < Ca-plagioclase < Na-plagioclase.

2. This study supports Sherman's (1952), Dennen and Anderson's (1962), Laughnan's (1964) and Augusthitis and Otteman's (1966) observations that early stages of weathering are indicated by oxidation of ferrous iron to form oxidized iron phases, such as: hematite, maghemite and goethite.

3. The dissolution of rocks and minerals during the first thirty minutes of contact between the solid and the solution is relatively fast. The solutions approach "stability" (term used in this study) during these 30 minutes. Similar observations were made by Huang and Keller (1970).

4. The data of this study suggest that as a result of the dissolution a thin alumino-silicate layer forms on the solid surface. Such a layer was suggested and discussed by: Wollast (1958), De-Vore (1958), Correns (1961) and Helgeson (1971). The dissolution mechanism through such a layer was proposed to be diffusion by Lyle (1943), Douglas and El-Shami (1967), Burkett (1970) and Burkett et al (1970). The data of the present research support this mechanism.

5. The solubility of glasses was found to be a function of weight solid/volume solution (Burkett, 1970). The present study confirms this fact and extends it to be true also for basalts.

The conclusions of this research which are unique are:

1. In early stages of basalt weathering a new iron bearing phase is observed. It probably contains mainly goethite and is called here Fe-mineral. The amount of Fe-mineral increases with weathering time.

2. A basalt that weathers in an arid environment becomes depleted of silica, sodium, potassium and alumina and becomes relatively enriched in iron, calcium, magnesium, titanium, cobalt, chromium, and phosphate.

3. The most applicable weathering indicies for basalts located in arid environments are:
   a. ΔWI_{Fe}
   b. $\Delta \leq Fe$
   c. $\Delta(Fe^{+2}/Fe^{+3})$
   d. Parker's modified index
   e. Jenny's index

4. Caliche that is found in cracks and vesicles of basalts in dry environments may result from weathering.

5. Magnetite weathers in arid climates in the following sequence: magnetite $\longrightarrow$ goethite $\longrightarrow$ hematite, with the possibility of forming β-goethite as an intermediate product.

6. The experimental results of this investigation show that:
   (a) In dry areas where potential evaporation > rainfall, weathering of basalts may produce calcite, Mg-montmorillonite, sepiolite, attapulgite and ferric-oxyhydroxide.
   (b) In dry areas where potential evaporation=rainfal weathering of basalts may produce: iron oxyhydroxides and probably clays but no calcite.

PLATE A

Photomicrograph 1: Low rate leaching experiment. The column on the left contains 10g basalt (Car -9), 270-400 mesh in size and is leached at an average rate of 135 ml of distilled water/day. The column on the left contains 10g glass (Mac-4), 270-400 mesh in size and is leached at an average rate of 65 ml of distilled water/day. The column is 1 cm in diameter.

Photomicrograph 2: Low rate leaching experiment. The top of the column leaching glass, containing the reddish brownish iron-rich specks that developed during this experiment. The column is 1 cm in diameter.

PLATE B

Photomicrograph 1: Low rate leaching experiment. The bottom of the column containing the leaching glass. The column is rich in the iron rich grains. The grains become darker with time, as can be observed from the large grain in the center of the column. The new grown material has a light red color, but the older grain has a darker reddish-brownish color. The column is 1 cm in diameter.

PLATE C

Photomicrograph 1: Glass (Mac-4), 270-400 mesh is size, x 3000 (Scanning Electron Microscope), used in the alternate wetting and drying experiment.

Photomicrograph 2: x 6000 of the glass used in the alternately wetting and drying experiments.

PLATE D

Photomicrograph 1: S. E. M. x5000 of the glass after three periods of wetting and drying (249 hours). The white specks result from the soluble cations that have been drawn to the surface by capillary forces.

Photomicrograph 2: (S. E. M. x3000). Beginning of crust formation after four periods of wetting and drying and an accumulative time of 456 hours.

Photomicrograph 3: (S. E. M. x3000). The growing of the crust on glass sharks and the accumulation of soluble specks, after the fifth period of wetting and drying (2045 hours).

PLATE E

Photomicrograph 1: (S. E. M. x3000). The crust formed at the end of the fifth wetting and drying period (2045 hours), washed for 24 hours in distilled water to remove the soluble portion of the crust.

Photomicrograph 2: (S. E. M. x5000) of photomicrograph 1.

Photomicrograph 3: (S. E. M. x5000). The crust formed after five periods of wetting and drying (unwashed). The soluble specks can be seen clearly.

PLATE F

Photomicrograph 1: (S. E. M. x5000). Crust developed on glass after five periods of wetting and drying (2045 hours), washed with distilled water and diluted hydrochloric acid to remove soluble ions and carbonates.

The elongated grains are clay minerals probably mainly sepiolite (Grum, 1953).

Photomicrograph 2: (S.E.M. x6000). Higher magnification of photomicrograph 1.

PLATE G

Photomicrograph 1: (S. E. M. x 3000). The small amorphous reddish grains that developed on the bottom of the glass after five periods of wetting and drying (2045 hours).

Photomicrograph 2: S. E. M. x 10000 of photomicrograph 1.

PLATE A

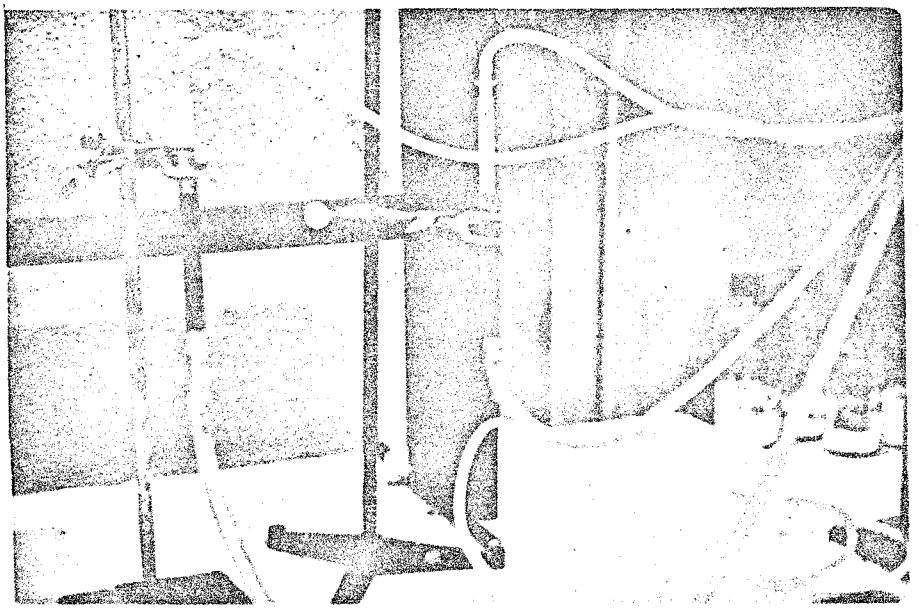

1

2

PLATE B

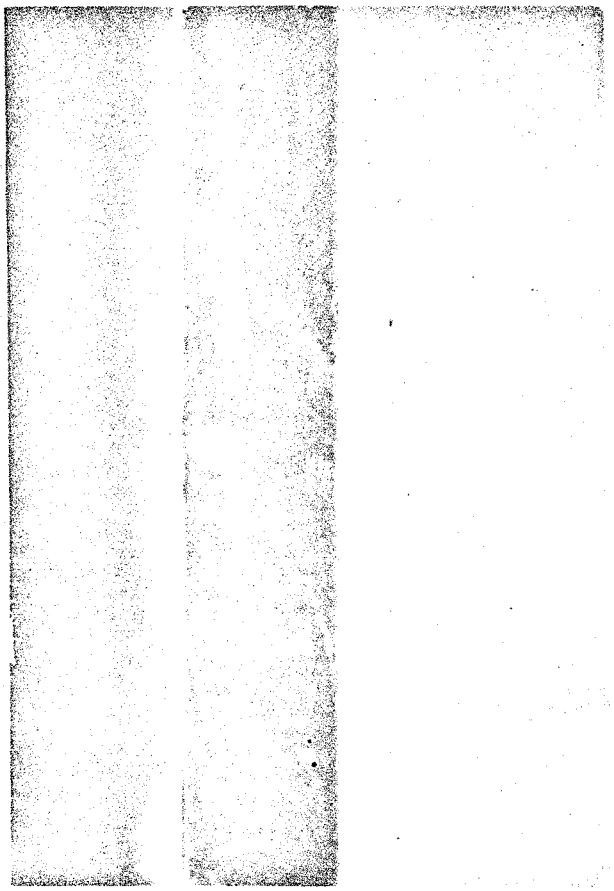

1

PLATE C

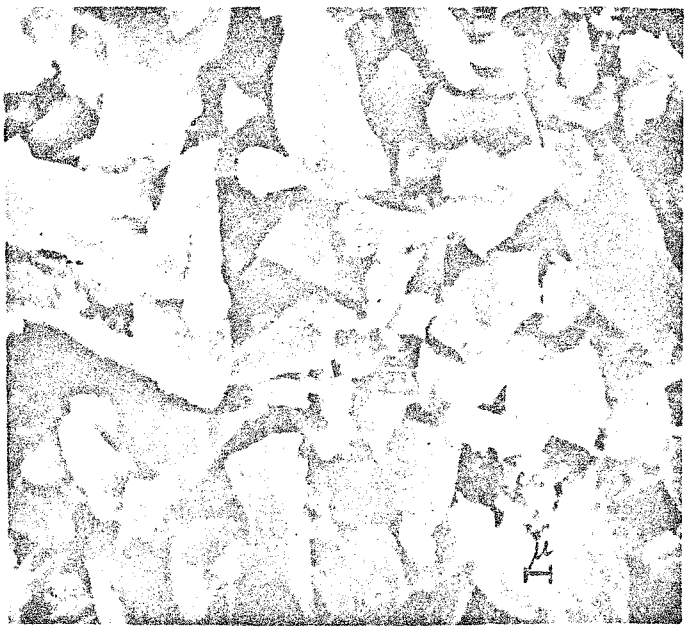

1

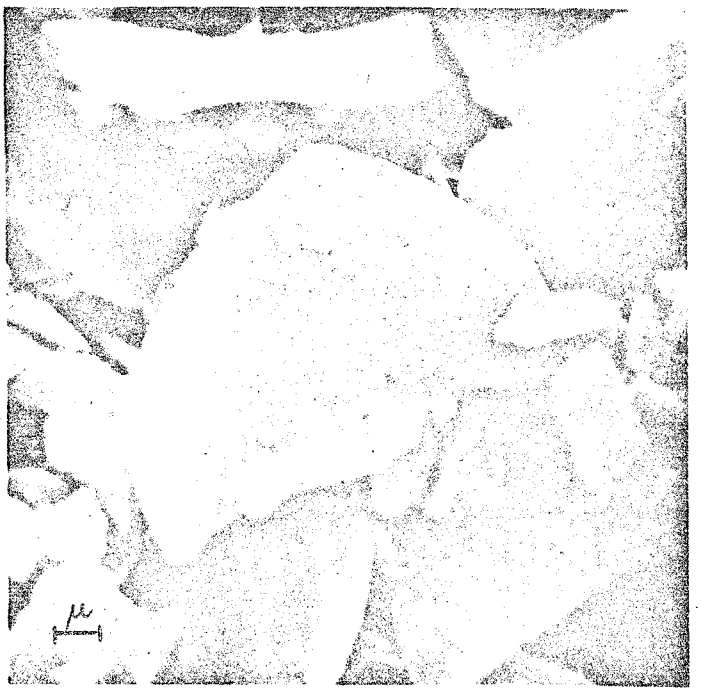

PLATE D

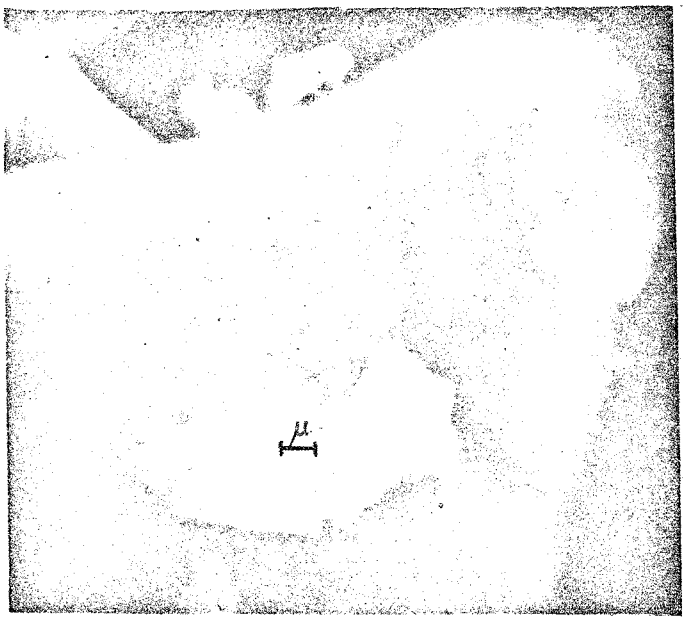

1

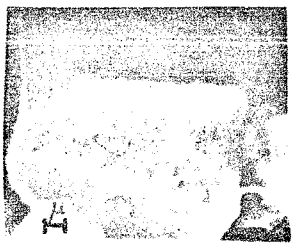

2

3

PLATE E

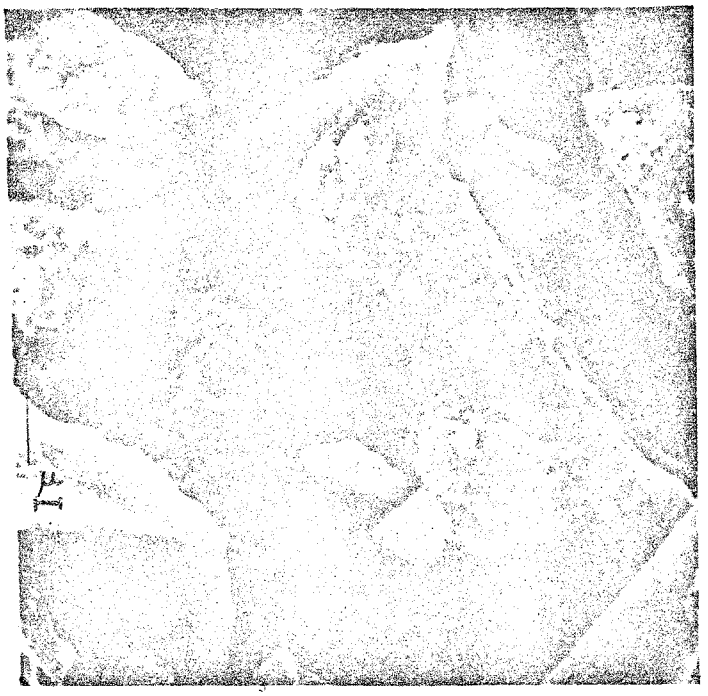

1

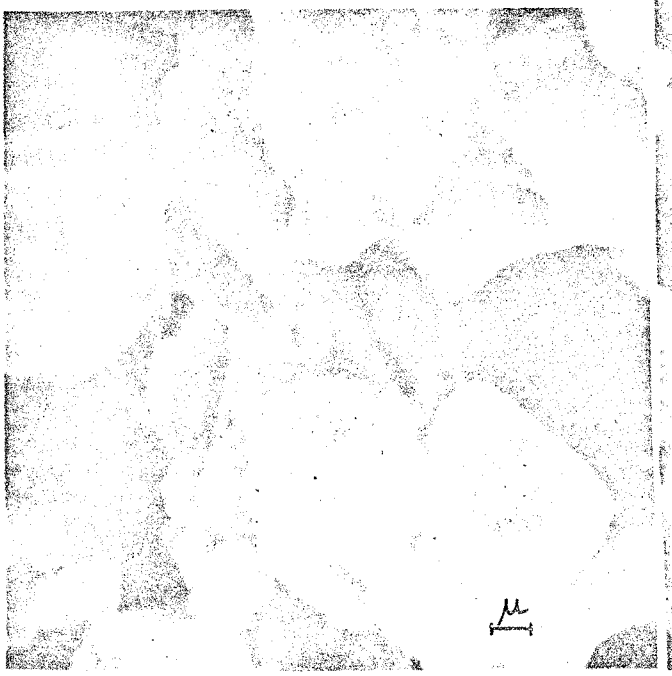

2

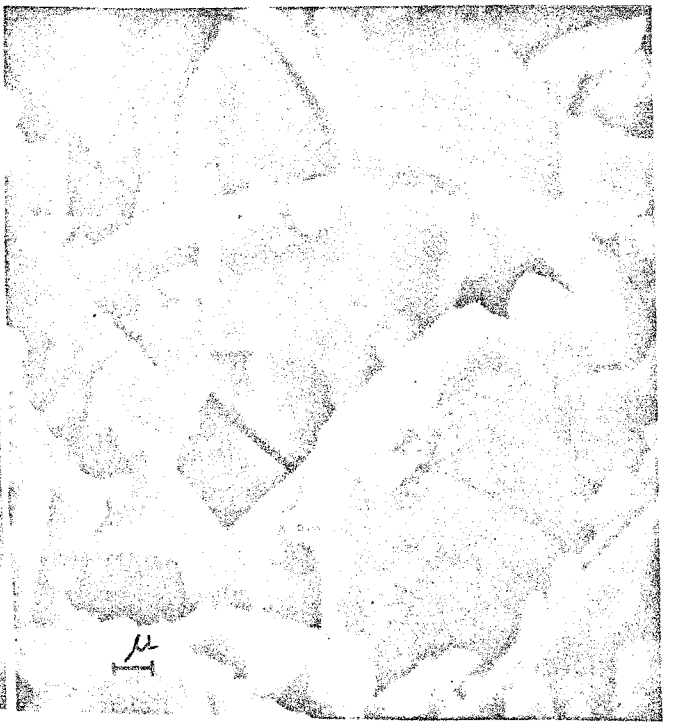

3

PLATE F

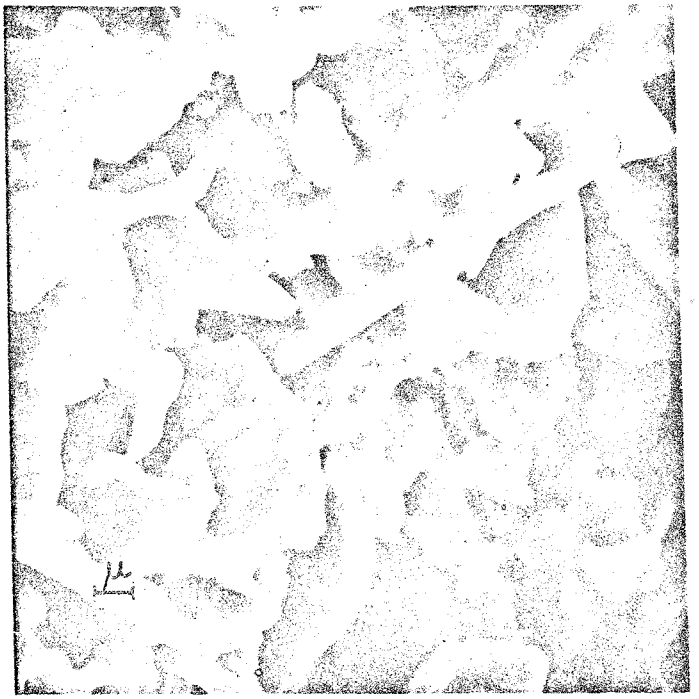

1

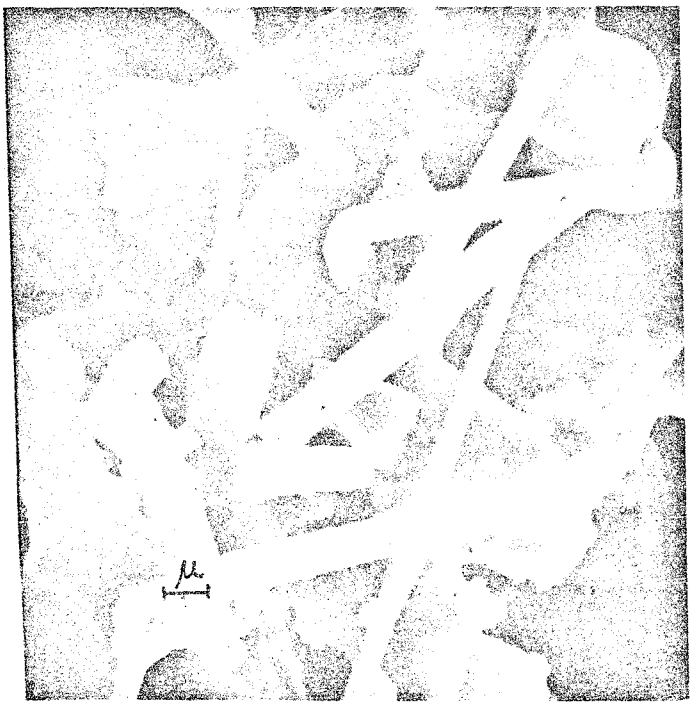

2

PLATE G

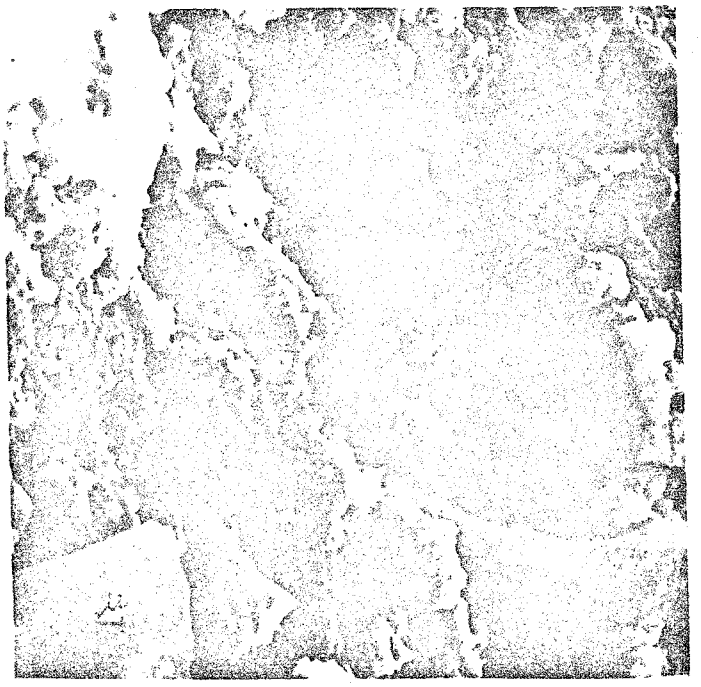

1

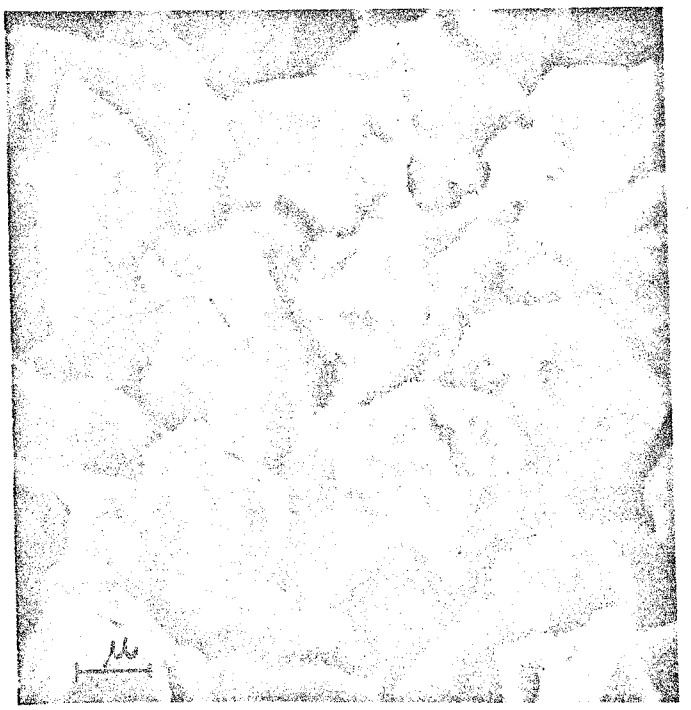

2

APPENDIX A

ANALYTICAL PROCEDURES

Thin Sections

Thin sections from the five selected flows in the Black Mountains-Santo Tomas region were sliced perpendicular to the weathered surface (111 sections). They were cut from the weathered surface and the fresh core of the sampled rock boulders with special effort to preserve the altered surface. The thin sections were examined with binocular and petrographic microscopes and point counts of mineralogy were made. The groundmass was very fine grained, necessitating moving the point counter in steps of 0.1 millimeter. When examining thin sections containing fresh rock the starting point was randomly chosen and 600-700 points were counted. When the weathered surface was inspected, the point counting was done by traversing the entire weathered area as closely as possible. Points counted did not exceed 700 in the case of weathered samples.

The reproducibility of the point counting was established by counting a weathered surface and a nonweathered thin section from the San Miguel flow twice each on different dates. The coefficient of variation was as follows:

Non weathered:	Vs	=	0.92%
	Plag.	=	0.75%
	Ol	=	1.27%
	Gl+Au+Mag	=	2.23%
	Idd	=	0.49%
	Fe-min.	=	0.26%

Weathered surface:	Vs	=	0.69%
	Plag.	=	0.83%
	Ol	=	1.52%
	Gl+Au+Mag	=	1.93%
	Idd	=	0.67%
	Fe-min.	=	0.42%

To establish whether the number of thin-sections point counted is statistically sufficient, for the mean composition of WI_{Fe} to be within 95 percent confidence, the Student's t-test was performed. The number of samples required for this confidence was calculated using the formula given by Krumbein and Grayhill (1965):

$$N = (st/d)^2$$

where: N is the number of required samples,

s is the standard deviation

t is the tabulated value of the t distribution at a half probability of 0.025 for the appropriate degrees of freedom (tables Dixon and Massey, 1957)

d is the deviation from the mean

The results of these calculations indicate that the number of samples point counted always exceeded the required N.

Scanning Electron Microscopy (SEM)

Some scanning electron microphotographs were made by Mr. C. W. Walker using the facilities at Louisiana State University. The purpose of this procedure was to identify any changes in the experimentally leached surfaces, such as growth of very small quantities of new phases that could not be identified precisely by other methods.

X-ray Fluorescence

X-ray fluorescence analyses of sample-pellets were performed using a 8-position Norelco vacuum spectrograph. Counting was done on fixed time mode, and three previously analyzed basalts (Table 11) served as standards. Standard Car-9 was kept in one position of the spectrograph and was run prior to every set of seven unknowns, and the count rate of each unknown was divided by the count rate of Car-9 obtained with each set. Each standard and sample set were counted at least six times, and the ratios of counts/Car 9 counts were averaged.

Calibration curves were constructed using the data obtained for the three standards by the method described by Renault (1970). The x-ray fluorescence instrumental parameters are given in Table 12 .

To determine the reproducibility, ten pellets from one basalt sample were prepared and analyzed. The reproducibility is expressed as the coefficient of variation: $C.V. = \frac{\text{standard deviation} \times 100}{\text{mean}}$ and is listed in Table 13.

The residual fractions from the thin section preparation were coarse crushed (3.5-5 mesh) and hand picked to eliminate vesicle fillings, then fine ground (< 325 mesh) under acetone in an automatic mortar for 30 minutes. Undiluted briquettes were made according to Volborth's (1963) method and Renault's (1970) modification. For most samples the sample pellets were prepared in duplicate.

TABLE 11

Chemical and normal analyses of basalt standards

	Wet chemical analyses* (weight percent)		
	CAR-9	MAC-16	POT-11
SiO_2	51.07	49.93	44.00
TiO_2	1.58	1.38	2.35
Al_2O_3	17.65	16.62	14.76
Fe_2O_3	2.01	1.54	4.46
FeO	7.76	9.25	7.33
MnO	0.15	0.17	0.22
MgO	5.98	8.45	10.44
CaO	8.23	8.90	10.40
Na_2O	3.90	2.89	3.07
K_2O	1.21	0.75	1.40
P_2O_5	0.33	0.25	0.58
H_2O^+	0.02	0.02	0.65
H_2O^-	0.09	0.04	0.18
CO_2	0.00	0.00	0.00
S	0.0	0.0	0.0
Cr_2O_3	0.051	0.073	0.068
Ni	0.0095	0.0250	0.0225
Co	0.0058	0.0074	0.0070
Cu	0.0243	0.0181	0.0169
	100.07	100.32	99.96
Total iron as FeO	10.64	10.48	9.21

*Analysis by H. Wilk; total iron by L. Brandvold

TABLE 12

X-ray fluorescence instrumental parameters.

Element	kv/ma	tube/crystal	path (μ)	coll	det	B. L.	wid	det-kv	° peak	° Bk
SiO_2	40/27	Cr/Gyp	200	fine	P-10	8.2	6.5	1.62	55.99	57.70
Al_2O_3	50/38	W/Gyp	200	coarse	P-10	0.5	2.5	1.47	66.64	69.20
Na_2O	50/27	Cr/Gyp	100	coarse	nat. gas	4.5	13.5	2.48	103.30	---
K_2O	40/27	Cr/Gyp	100	coarse	P-10	8.2	6.5	1.56	38.54	27.48
FeO	30/15	W/Qz	200	coarse	P-10	11.0	20.0	1.60	33.90	---
CaO	50/40	W/Qz	500	coarse	P-10	15.0	20.0	1.60	60.30	57.60
MgO	50/27	Cr/Gyp	100	coarse	nat.gas	5.8	8.0	2.48	81.30	76.75
TiO_2	50/40	W/Qz	500	coarse	P-10	15.0	20.0	1.60	48.54	46.00
P_2O_5	40/27	Cr/Gyp	200	coarse	P-10	8.8	7.5	1.60	47.84	---
Cr_2O_5	50/40	W/Qz	no vac.	coarse	P-10	2.3	7.0	1.50	40.05	41.80
Ni	50/40	W/Qz	no vac.	coarse	P-10	6.8	10.0	1.56	28.70	27.40
Co	50/40	W/Qz	no vac.	coarse	P-10	0.5	18.5	1.54	31.04	28.35

TABLE 13

X-ray fluorescence instrumental precision

	% Maximum	% Minimum	% Mean	S. D.	% C of V
SiO_2	48.13	47.46	47.70	0.23	0.5
Al_2O_3	22.12	19.63	20.74	0.86	4.1
Na_2O	3.97	3.71	3.81	0.10	2.7
K_2O	1.70	1.66	1.67	0.01	0.8
FeO	8.26	7.75	8.03	0.17	2.3
CaO	9.17	8.91	9.05	0.09	1.0
MgO	8.00	7.75	7.89	0.09	1.1
TiO_2	2.09	2.02	2.05	0.02	1.2
P_2O_5	0.42	0.38	0.40	0.01	3.5
Cr_2O_5	0.045	0.040	0.044	0.002	4.1
Ni	0.034	0.014	0.024	0.007	28.6
Co	0.005	0.004	0.005	0.001	2.8

X-ray Diffraction

X-ray diffraction techniques were used to determine the mineralogical phases present in the natural samples and the mineralogical changes in the leached rock, glass and minerals. A Norelco diffractometer equipped with a copper target and a nickel filter was used.

The Debye-Sherrer film technique

To identify new phases produced by the weathering experiments, the Debye-Sherrer film technique was used. This method makes use of a cylindrical film, whose axis coincides with the rotation axis of the sample and is normal to the beam. The beam enters between the ends of the film and passes through the camera by way to two symmetrically siturated and diametrically opposite holes in the film. As a result, the front- and back-reflection arc are separately grouped on the film, the front reflection about one hole and the back reflection about the other (Straumanis position).

The proper corrections for the shrinkage and expansion of the film were made, and using the formula $\frac{S}{4} = \theta$, where S is the distance between a pair of arcs, the diffraction angle θ was obtained.

Other Chemical Analytical Methods

Chemical analysis were made to determine the chemical composition of the basalt, the glass and the minerals used, and to establish the composition of the leached solutions.

Colorimetric, gravimetric, volumetric and atomic absorption spectrometric methods were used.

Colorimetric and gravimetric methods

Colorimetric methods were used to determine the concentration of alumina and silica in solution; alumina by the aluminon method and silica by the molybdosilicate method (Standard Methods 1961). Silica and alumina in silicates were determined by accurate gravimetric analyses and titanium in rock and solution was determined by the peroxide colorimetric method as described by Bennett and Hawley (1965).

Volumetric methods

The amount of ferrous iron present in rocks was found by titrating against potassium dichromate (Bennett and Hawley, 1965). The concentration of the ferric iron was determined by subtracting the amount of Fe^{+2} from the total iron concentration. The concentration of bicarbonate ions in solution was established by titrating against sulfuric acic (Standard Methods 1961).

Atomic absorption spectroscopy

The ions analyzed by the atomic absorption method and the operating conditions of the Perkin-Elmer 303 spectrometer used are given in Table . The techniques used were adopted from the Perkin-Elmer Analytical Methods book.

TABLE 14

Atomic Absorption Instrumental Parameters

Element	Wave length (A^o)	Cathode current (mA)	Range	Slit (mm)	Fuel	Oxidant
Na	5890	15	Vis	1	C_2H_2	Air
Mg	2852	10	U. V.	1	"	"
K	7665	30	Vis	1	"	"
Ca	4227	20	Vis	1	"	"
Fe	2483	35	U. V.	0.3	"	"
Cu	3247	20	U. V.	1	"	"
Sr	4607	20	Vis	1	"	"
Ba	5536	30	Vis	0.3	"	N_2O
Zn	2138	15	U. V.	3	"	Air
V	3183	40	U. V.	1	"	"
Ga	2874	25	U. V.	1	"	"
Mo	6045	30	U. V.	1	"	N_2O
Ag	3281	30	U. V.	1	"	Air
Pb	2830	40	U. V.	1	"	"
Cd	2288	10	U. V.	1	"	"
Mn	2795	20	U. V.	0.3	"	"
Co	2407	30	U. V.	0.3	"	"
Ni	2320	25	U. V.	0.3	"	"
Cr	3579	30	U. V.	1	"	"
Li	6708	25	Vis	1	"	"

Vis - visable spectrum; U. V. utraviolet spectrum

Boling burner head used throughout.

pH meter

pH of experimental solutions was measured on an Orion research pH meter model 801 digital pH. The precision was $\pm$0.1 pH units.

Concentration by Ion Exchanger

Solutions obtained from experiments were often too dilute to be analyzed and concentration was necessary. To determine the effect of concentrating mechanisms, a standard solution was prepared, and concentrated ten fold by evaporation and by using an ion exchanger. The results are listed in Table , and indicate that for all the analyzed elements excluding silica and alumina the use of the ion exchanger yielded relatively better results, therefore bicarbonate, pH, silica and aluminum were determined prior to the concentration.

The ion exchanger used was: Bio-Rad, AG50W x 10 100-200 mesh (hydrogen form).

TABLE 15

Analyses of a 10X concentrated standard solution by evaporation and by an ion exchanger

Element	Standard (ppm)	Evaporated Solution	Acidic Solution from Ion Exchanger	Sample Solution leached by Ion Exchanger
K	0.5	6.90	5.25	0.00
Na	5.0	47.50	48.75	0.00
Ca	6.0	51.70	54.00	0.00
Mg	0.5	2.08	3.60	0.00
Fe	1.0	10.40	10.20	0.00
Cu	0.2	2.40	2.00	0.00
Cr	0.2	9.50	3.90	0.00
Ti	0.2	0.00	0.00	0.00
Ni	0.2	2.20	1.80	0.00
Mn	0.2	1.70	2.10	0.00
Ba	0.1	1.50	0.80	0.00
Sr	0.1	0.00	0.00	0.00
Rb	0.1	0.00	0.00	0.00
Li	0.1	1.30	0.75	0.00
SiO_2	2.0	4.60	0.52	1.04
Al_2O_3	2.0	5.98	0.02	0.03

APPENDIX B

MINERALOGICAL AND CHEMICAL RESULTS

Table 16 lists the mineralogical composition of weathered and nonweathered samples of the five studied flows as determined by point counting. In this table the following symbols were used:

Vs	=	vesicles	Gl	=	glass
Plag	=	olivine	Au	=	augite
idd	=	iddingsite	Mag	=	magnetite
			Fe-min	=	Fe-mineral

$$WI_{Fe} = \frac{100 \times \text{Fe-mineral}}{100 - (\text{Vs} + \text{Plag} + \text{Fe-mineral}}$$

Table 17 lists the chemical composition of weathered and nonweathered samples of these flows as determined by x-ray fluorescence. Table 18 lists the chemical analysis of solutions from short term leaching experiments, Table 19 gives the chemical analysis of washing solutions of the alternate wetting and drying experiments, and Table 20 lists the x-ray data of calcite formed on wetting and drying glass in comparison to natural calcite.

TABLE 16

Mineralogic Composition of Flows

Santo Tomas - 1: Unweathered

Sample	%Vs	%Plag.	%Ol	%Gl+Au +Mag	%Idd	%Fe-min.	WI_{Fe}
1- 2n	3.21	32.40	9.37	54.61	0.00	0.41	0.64
1- 3n	2.71	34.46	9.02	53.82	0.00	0.00	0.00
1- 4n	3.25	31.70	10.08	54.58	0.00	0.38	0.59
1- 7n	2.98	35.68	9.16	51.70	0.00	0.47	0.77
1- 8n	4.05	32.96	8.47	54.38	0.00	0.14	0.22
1- 9n	4.13	31.83	9.48	54.30	0.00	0.26	0.41
1-13n	5.26	30.50	7.86	55.94	0.00	0.36	0.56
1-14n	3.82	33.45	10.03	52.53	0.00	0.17	0.27
1-15n	3.46	33.21	8.01	55.32	0.00	0.00	0.00
1-26n	2.25	32.33	10.12	54.96	0.00	0.33	0.507
10- 1n	4.46	32.25	8.53	54.57	0.00	0.19	0.30
6- 1n	5.46	31.52	9.84	52.85	0.00	0.32	0.51
Mean	3.77	32.70	9.164	54.13	0.00	0.25	
Mean excluding Vs		33.99	9.52	56.23	0.00	0.26	

Santo Tomas - 1: Weathered

Sample	%Vs	%Plag.	%Ol	%Gl+Au +Mag	%Idd	%Fe-Min.	WI_{Fe}
1- 1w	1.01	29.84	9.26	55.34	0.00	4.56	7.06
1- 5w	0.00	35.06	8.74	52.10	0.00	4.09	6.72
1- 6w	0.93	32.63	8.98	52.74	0.00	4.72	7.65
1-10w	1.57	33.53	9.54	51.04	0.00	4.33	7.15
1-11w	1.06	31.87	10.02	51.84	0.00	5.21	8.42
1-16w	0.00	34.16	7.49	53.82	0.00	4.53	7.39
1-17w	0.00	35.67	10.76	49.76	0.00	3.81	6.29
1-18w	0.67	30.83	8.03	55.91	0.00	4.57	7.15
1-19w	0.83	32.07	9.26	53.72	0.00	4.11	6.52
1-20w	0.24	34.29	10.49	51.16	0.00	3.83	6.21
10- 2w	1.21	33.01	7.24	53.53	0.00	5.02	8.26
6- 2w	0.98	32.24	10.41	52.92	0.00	3.46	5.46
Mean	0.71	32.93	9.19	52.83	0.00	4.35	
Mean excluding Vs		33.17	9.26	53.21	0.00	4.37	

Santo Tomas - 2: Unweathered

Sample	%Vs	%Plag.	%Ol	%Gl+Au +Mag	%Idd	%Fe-min.	WI_{Fe}
7- 6n	6.28	32.40	9.54	51.37	0.00	0.41	0.67
7- 7n	7.52	27.87	10.06	54.55	0.00	0.00	0.00
7- 8n	5.92	26.82	9.83	57.44	0.00	0.00	0.00
7- 9n	7.85	35.40	9.97	46.48	0.15	0.16	0.28
7-10n	6.43	33.92	10.23	49.21	0.00	0.21	0.35
7-11n	7.09	28.34	7.93	56.63	0.00	0.00	0.00
7-12n	4.62	31.77	11.13	51.96	0.21	0.32	0.505
4- 1n	7.13	26.56	8.48	57.84	0.00	0.00	0.00
5- 1n	4.08	33.27	10.15	52.36	0.00	0.14	0.22
2- 1n	7.49	35.32	9.41	47.39	0.13	0.26	0.46
Mean	6.44	31.17	9.67	52.52	0.049	0.15	
Mean excluding Vs		33.31	10.33	56.13	0.051	0.16	

Santo Tomas - 2: Weathered

Sample	%Vs	%Plag.	%Ol	%Gl+Au +Mag	%Idd	%Fe-min.	WI_{Fe}
7- 1w	2.27	31.24	9.76	54.28	0.00	2.45	3.83
7- 2w	0.00	34.92	10.24	51.49	0.18	3.16	5.10
7- 3w	1.79	30.52	8.63	56.21	0.00	2.84	4.38
7- 4w	3.94	37.46	10.21	45.04	0.26	3.10	5.59
7- 5w	3.47	35.76	9.83	47.78	0.19	2.96	5.12
7-13w	1.27	33.17	10.18	52.14	0.00	3.24	5.20
7-14w	2.08	29.31	9.02	55.49	0.00	2.66	4.03
4- 2w	1.36	34.25	9.93	50.88	0.36	3.23	5.28
5- 2w	0.00	28.71	9.64	58.99	0.00	4.01	5.96
2- 2w	0.00	31.06	8.83	56.85	0.00	3.27	4.98
Mean	1.62	32.64	9.63	52.92	0.099	3.10	
Mean excluding Vs		33.18	9.79	53.79	0.1	3.15	

Santo Tomas - 3: Unweathered

Sample	[illegible]s	%Plag.	%Ol	%Gl+Au +Mag	%Idd	%Fe-min.	WI_{Fe}
3- 3 n	19.96	29.82	12.12	38.11	0.13	0.13	0.26
3- 4an	9.02	24.42	9.27	57.02	0.00	0.26	0.39
3- 4bn	10.67	32.03	8.52	48.78	0.00	0.00	0.00
3- 8 n	10.94	25.09	10.07	53.24	0.33	0.33	0.52
3- 9 n	21.46	30.41	12.26	35.88	0.00	0.00	0.00
[illegible]	24.[illegible]	27.36	10.28	35.60	0.21	0.00	0.00
[illegible]	10.64	31.54	11.13	46.69	0.13	0.00	0.00
9- 1 n	8.25	26.67	9.68	54.68	0.24	0.48	0.74
9- 2 n	12.16	25.88	8.78	53.05	0.00	0.14	0.23
Mean	14.37	28.13	10.23	46.99	0.1	0.15	
Mean excluding		32.85	11.94	54.88	0.12	0.18	

Santo Tomas - 3: Weathered

Sample	%Vs	%Plag.	%Ol	%Gl+Au +Mag	%Idd	%Fe-min.	WI_{Fe}
3- 1w	2.78	26.73	10.47	56.92	0.61	2.48	3.65
3- 2w	2.49	33.89	11.46	48.28	1.19	2.69	4.41
3- 5w	1.26	34.69	13.73	46.58	0.48	3.25	5.34
3- 6w	0.97	27.42	12.59	57.10	0.00	1.93	2.77
3- 7w	2.41	29.76	8.72	55.68	1.26	2.16	3.29
3-10w	1.07	30.56	11.29	53.54	0.58	2.97	4.54
3-11w	3.22	32.41	7.94	54.06	0.27	2.10	3.37
8- 3w	0.00	33.04	12.37	50.18	0.96	3.45	5.43
8- 4w	3.96	30.26	8.46	55.08	0.00	2.23	3.51
9- 3w	1.72	29.06	12.78	51.63	1.76	3.05	4.61
9- 4w	0.00	25.49	10.94	60.54	0.28	2.76	3.85
Mean	1.81	30.30	10.98	53.61	0.67	2.64	
Mean excluding Vs		30.86	11.18	54.60	0.68	2.69	

San Miguel : Unweathered

Sample	%Vs	%Plag.	%Ol	%Gl+Au +Mag	%Idd	%Fe-min.	WI_{Fe}
2n	11.09	33.64	16.25	36.77	1.86	0.4	0.73
3n	10.17	30.89	14.67	42.02	1.69	0.56	0.96
4n	14.38	42.85	8.59	32.55	0.91	2.73	1.74
7n	12.46	35.73	12.17	38.65	0.53	0.46	0.89
8n	6.91	32.63	9.33	49.73	0.60	0.79	1.33
9n	11.14	40.77	14.28	32.72	0.46	0.63	1.32
Mean	11.025	36.09	12.55	38.74	1.008	0.595	
Mean excluding Vs		40.56	14.10	43.54	1.13	0.67	only rock

San Miguel : Weathered

Sample	%Vs	%Plag.	%Ol	%Gl+Au +Mag	%Idd	%Fe-min.	WI_{Fe}
1w	5.00	30.29	10.05	46.19	3.78	4.70	7.83
5w	3.24	37.35	14.57	38.85	1.94	4.05	7.58
6w	0.00	48.24	8.60	38.49	0.83	3.83	7.99
10w	1.05	38.08	12.47	41.95	1.14	5.31	9.56
11w	0.00	46.30	11.73	36.23	1.38	4.36	8.84
12w	0.93	40.00	16.96	36.34	0.98	4.80	8.85
13w	1.49	33.62	13.41	45.77	1.93	3.79	6.20
Mean	1.67	39.12	12.54	40.58	1.71	4.45	
Mean excluding Vs		39.79	12.75	41.27	1.74	4.52	

Black Mountain - 6: Unweathered

Sample	%Vs	%Plag.	%Ol	%Gl+Au +Mag	%Idd	%Fe-min.	WI_{Fe}
5n	9.84	32.76	13.42	43.55	0.21	0.21	0.37
6n	9.96	33.49	12.42	43.96	0.00	0.18	0.32
8n	12.25	42.34	10.37	34.77	0.00	0.27	0.60
10n	16.43	37.62	8.39	37.30	0.00	0.26	0.57
11n	19.54	36.09	9.39	34.98	0.00	0.00	0.00
Mean	13.60	36.46	10.79	38.91	0.04	0.18	
Mean excluding Vs		42.20	12.50	45.04	0.05	0.21	

Black Mountain - 6: Weathered

Sample	%Vs	%Plag.	%Ol	%Gl+Au +Mag	%Idd	%Fe-min.	WI_{Fe}
1w	1.34	41.63	10.99	44.55	0.00	1.49	2.68
2w	0.82	45.02	14.21	38.69	0.00	1.26	2.38
3w	2.43	39.46	12.65	43.42	0.00	2.02	3.60
4w	1.76	40.70	11.89	43.57	0.12	1.96	3.52
7w	1.92	38.81	9.76	46.94	0.00	2.57	4.53
9w	0.00	42.59	13.43	39.82	0.00	3.17	5.95
12w	2.23	42.25	11.60	41.30	0.18	2.45	4.62
Mean	1.50	41.64	12.08	42.61	0.04	2.13	
Mean excluding Vs		42.27	12.26	42.26	0.04	2.16	

TABLE 17

Chemical Analyses of Flows:

Nonweathered (n) and Weathered (w)

Santo Tomas - 1

Sample	%SiO_2	%Al_2O_3	%FeO	%CaO	%TiO_2	%MgO	%Na_2O	%K_2O	%P_2O_5	NiO (ppm)	CoO (ppm)	Cr_2O_3 (ppm)	Total
1- 3n	47.92	15.60	9.23	9.49	2.23	8.75	3.61	1.70	0.44	388	64.53	51.18	98.97
1- 6w	46.66	16.70	9.86	9.78	2.35	9.74	2.83	1.54	0.47	348	74.80	63.40	99.93
1- 8n	47.31	17.65	8.92	9.54	2.20	8.43	3.43	1.72	0.47	573	51.64	51.08	99.67
1-17w	46.66	17.50	9.25	9.74	2.35	9.04	2.63	1.62	0.47	954	68.74	55.42	99.26
1-20n	47.08	16.31	9.75	10.49	2.43	9.23	2.70	1.37	0.60	289	79.82	61.80	99.96
1-23w	45.72	17.00	10.41	10.24	2.54	9.48	2.51	1.15	0.54	498	86.92	66.60	99.50
1-24n	46.35	18.63	8.51	10.02	2.29	8.98	3.08	1.71	0.52	368	75.26	57.20	101.09
1-29w	45.63	17.45	9.80	10.33	2.48	9.07	2.36	1.37	0.54	538	82.84	59.68	99.03
1-30w	46.46	16.44	9.42	9.91	2.45	8.91	2.90	1.35	0.55	---	81.88	51.25	98.39
1-31n	46.14	17.38	9.01	9.58	2.31	8.63	3.12	1.56	0.52	---	58.81	50.46	98.25
1-32w	45.48	16.65	9.86	9.99	2.43	9.74	2.69	1.35	0.54	---	81.16	55.66	98.73
1-33w	45.58	17.50	9.80	9.95	2.42	9.57	2.66	1.38	0.55	---	75.40	60.66	99.41
mean n	46.93	17.32	8.92	9.66	2.26	8.70	3.31	1.67	0.49	404	68.01	52.48	99.26
mean w	46.16	16.94	9.77	10.05	2.43	9.35	2.66	1.39	0.53	584	78.82	59.31	99.28

Santo Tomas - 2

Sample	%SiO_2	%Al_2O_3	%FeO	%CaO	%TiO_2	%MgO	%Na_2O	%K_2O	%P_2O_5	NiO (ppm)	CoO (ppm)	Cr_2O_3 (ppm)	Total
2- 3w	45.65	17.33	10.03	9.66	2.45	9.45	2.89	1.31	0.49	449	93.30	45.17	99.26
2- 8n	46.12	20.04	8.54	9.58	2.31	8.50	3.28	1.56	0.46	467	65.49	40.13	100.36
2-11n	47.09	16.16	9.53	9.41	2.22	9.58	3.16	1.52	0.44	358	64.68	43.56	99.11
2-13w	45.69	15.44	10.23	10.08	2.45	9.62	2.71	1.34	0.56	383	96.06	44.20	98.12
2-18w	45.70	16.68	10.29	9.41	2.35	10.01	2.70	1.38	0.45	366	83.22	49.45	98.97
2-21n	46.43	17.45	9.64	9.74	2.22	8.70	3.17	1.54	0.47	337	62.75	45.00	99.36
2-23n	47.61	16.12	9.16	9.41	2.26	8.74	3.52	1.53	0.41	335	73.02	46.20	98.67
2-25w	45.38	17.25	10.48	9.78	2.40	10.00	2.59	1.22	0.46	260	85.89	47.25	99.56
Meann	46.81	17.44	9.22	9.56	2.25	8.88	3.28	1.54	0.45	374	66.48	43.72	99.43
Meanw	45.60	16.68	10.26	9.73	2.41	9.77	2.72	1.31	0.49	365	89.62	46.52	98.97

Santo Tomas - 3

3- 1w	45.17	17.71	9.96	9.58	2.42	10.18	2.27	1.27	0.53	279	97.21	47.42	99.09
3- 3n	46.54	18.50	9.41	9.84	2.22	9.07	2.88	1.48	0.50	270	71.55	43.50	100.44
3- 5w	45.21	17.21	9.98	10.20	2.30	10.02	2.32	1.27	0.53	299	90.81	44.83	99.04
Meann	46.54	18.50	9.41	9.84	2.22	9.07	2.88	1.48	0.50	270	71.55	43.50	100.44
Meanw	45.19	17.46	9.97	9.89	2.36	10.10	2.30	1.27	0.53	289	94.01	46.13	99.07

San Miguel

Sample	%SiO_2	%Al_2O_3	%FeO	%CaO	%TiO_2	%MgO	%Na_2O	%K_2O	%P_2O_5	NiO (ppm)	CoO (ppm)	Cr_2O_3 (ppm)	Total
1w	46.25	17.83	9.57	9.16	1.74	10.00	2.13	1.36	0.48	338	115.99	53.50	98.52
7n	46.45	19.66	9.49	7.74	1.37	9.86	3.21	1.52	0.53	318	72.37	40.33	99.83
10n	46.95	19.00	9.03	8.32	1.69	9.13	2.96	1.51	0.53	299	52.50	48.40	99.12
12w	46.04	18.00	9.96	9.32	1.79	10.69	2.51	1.40	0.52	308	115.30	50.00	99.23
Meann	46.70	19.33	9.26	8.03	1.53	9.50	3.09	1.52	0.51	308	62.44	44.37	99.47
Meanw	46.14	17.92	9.77	9.24	1.77	10.35	2.32	1.38	0.50	323	115.65	51.75	99.89

Black Mountain - 6

2w	46.67	18.50	8.59	9.91	1.97	7.30	3.05	1.72	0.58	410	75.21	29.20	98.29
6n	48.13	19.56	8.22	10.16	1.89	7.08	3.61	1.93	0.39	309	68.00	27.33	100.97
7n	48.13	18.75	8.14	9.66	2.29	6.83	3.50	1.93	0.46	328	56.31	22.40	99.69
8n	47.92	18.25	8.23	9.58	2.33	7.00	3.39	1.95	0.48	377	59.61	27.16	99.13
Meann	48.06	18.85	8.20	10.13	2.17	6.97	3.50	1.94	0.44	238	61.31	25.63	100.26
Meanw	46.67	18.50	8.59	9.91	1.97	7.30	3.05	1.72	0.58	410	75.21	29.20	98.29

TABLE 18

Chemical analyses of short term experiments (in ppm):

Labradorite

Run	SiO_2	Al_2O_3	Na^+	K^+	Ca^{++}	Mg^{++}	HCO_3^-	pH
1(43hr)	2.94	0.30	3.35	1.30	3.10	0.11	14.00	6.86
2(84hr)	3.60	0.68	2.18	1.00	1.95	0.11	10.40	7.10
3(24hr)	1.68	0.42	1.67	0.60	0.95	0.07	4.40	6.80
4(120hr)	2.80	0.49	1.49	0.66	0.95	0.07	4.00	6.95
5(24hr)	1.70	0.22	1.45	0.74	0.90	0.07	4.04	6.25
6(24hr)	--	0.12	0.70	0.37	0.95	0.08	4.00	6.24
7(24hr)	1.22	0.00	0.45	0.58	0.86	0.00	4.40	5.97
8(1hr)	0.53	0.00	0.20	0.00	0.20	0.00	1.50	5.88
9(16hr)	0.89	0.00	0.43	0.00	0.48	0.00	2.00	5.95
10(16hr)	0.63	0.00	0.56	0.00	0.20	0.00	2.13	6.33
Heated	3.28	0.00	0.42	0.00	0.16	0.00	2.33	6.40

Magnetite

Run	$\leq Fe$	HCO_3^-	pH
1(16hr)	11.80	21.00	7.50
2(120hr)	21.50	14.80	6.80
3(20hr)	3.90	12.80	7.21
4(30hr)	0.60	5.48	6.07
5(24hr)	0.60	4.43	6.14
6(1hr)	0.70	1.24	5.88
7(16hr)	0.18	1.00	5.92
8(6hr)	0.10	1.33	5.85
Heated	0.85	15.00	6.22

Augite

Run	SiO_2	Al_2O_3	Na^+	K^+	Ca^{++}	Mg^{++}	$\leq Fe$	HCO_3^-	pH
1(43hr)	9.82	0.07	1.82	0.9	1.75	1.00	0.20	14.00	6.46
2(84hr)	2.72	0.27	1.87	1.1	1.45	0.59	0.40	8.80	6.40
3(24hr)	0.45	0.45	1.45	0.8	0.75	0.05	0.10	3.20	6.42
4(120hr)	0.98	0.61	1.45	0.46	1.00	0.10	0.10	2.00	6.61
5(48hr)	0.68	0.23	1.40	0.30	0.65	0.12	0.00	4.00	6.40
Heated	0.80	0.00	1.27	0.00	0.16	0.08	0.10	1.53	6.18

Glass (10 g in 100 cc H_2O)

1(44hr)	9.36	0.28	15.50	3.80	3.75	3.25	0.80	32.20	7.34
2(84hr)	3.19	0.79	5.16	9.80	3.65	2.45	2.00	30.20	7.34
3(24hr)	3.16	0.89	2.15	2.60	1.80	0.46	2.80	10.80	6.91
4(120hr)	6.94	0.42	2.67	4.20	3.12	1.07	1.80	15.20	7.47
5(24hr)	2.80	0.35	2.48	1.56	0.95	0.29	0.50	7.20	6.65
6(24hr)	2.78	0.00	2.40	0.70	3.65	0.09	0.20	5.70	6.29
7(24hr)	2.80	0.00	0.70	0.10	4.58	0.00	0.20	10.40	6.15
8(1hr)	2.84	0.00	0.60	0.00	0.38	0.49	0.20	6.80	6.90
9(16hr)	2.07	0.00	0.18	0.00	0.28	0.24	0.00	3.00	6.19
10(16hr)	2.38	0.00	0.23	0.00	0.31	0.36	0.00	4.13	6.51
Heated	3.26	0.00	0.53	0.00	0.28	0.69	0.00	5.67	6.65

Glass (3g in 100 cc H_2O

1(42hr)	4.81	0.35	3.37	0.8	2.35	1.48	0.00	20.80	7.13
2(84hr)	7.91	0.86	3.08	0.8	1.95	0.98	1.80	16.40	7.25
3(24hr)	2.47	0.28	2.73	0.6	1.85	0.22	1.80	6.00	6.75
4(120hr)	5.13	0.29	2.78	0.34	1.50	0.43	1.00	10.00	7.13
5(24hr)	1.84	0.42	1.28	0.12	0.82	0.13	0.80	5.60	6.66
6(24hr)	2.26	0.22	1.78	0.46	1.50	0.20	0.00	9.00	6.21
7(24hr)	1.11	0.16	1.28	0.53	1.47	0.00	0.00	5.00	6.10
8(1hr)	1.24	0.00	0.34	0.00	0.22	0.14	0.05	2.33	6.24
9(16hr)	0.82	0.00	0.18	0.00	0.28	0.11	0.17	2.00	5.91
10(6hr)	0.96	0.00	0.49	0.00	0.20	0.12	0.04	2.67	6.31

Olivine

Run	SiO_2	Al_2O_3	Ca^{++}	Mg^{++}	$\lesssim Fe$	HCO_3	pH
1(24hr)	11.97	0.84	2.20	6.25	0.00	40.40	8.55
2(84hr)	8.86	0.00	0.90	4.40	0.00	32.80	8.02
3(24hr)	4.84	0.13	0.68	1.57	0.30	12.80	7.71
4(40hr)	6.76	0.24	1.10	3.00	0.40	20.80	8.08
5(57hr)	5.53	0.00	0.36	0.00	0.00	12.00	6.72
Heated	6.89	0.00	0.00	3.22	0.40	16.60	7.13

TABLE 19

Concentration (mg ion/ 1000 g sample) of Washing Solutions of Alternate Wetting and Drying Experiments
Sample = Basalt Car-9

ions	30 hr	97 hr	145 hr	384 hr	668 hr
SiO_2	17.10	31.98	8.24	6.80	14.19
Al_2O_3	0.49	3.58	6.67	8.25	1.56
Na^+	20.60	37.50	113.24	61.20	13.86
K^+	6.30	9.53	36.60	8.64	0.00
Ca^{++}	37.20	117.90	77.85	39.00	20.70
Mg^{++}	1.98	5.74	7.60	3.60	5.53
$Fe^{+2}+Fe^{+3}$	0.00	1.85	0.00	2.40	4.15
Ni^{+2}	0.00	0.00	0.12	0.12	0.00
HCO_3^-	----	184.50	336.60	----	----
pH	----	6.96	7.49	----	3.70

Sample = Glass Mac-4

ions	30 hr	152 hr	249 hr	456 hr	2045 hr
SiO_2	15.71	42.73	253.15	43.79	3.67
Al_2O_3	1.09	3.74	16.53	1.92	0.00
Na^+	32.81	267.27	168.80	156.40	23.75
K^+	7.07	15.27	23.11	3.68	0.00
Ca^{++}	17.07	80.15	115.55	234.60	2.50
Mg^{++}	7.00	17.57	26.84	6.07	0.00
$Fe^{+2}+Fe^{+3}$	1.01	5.35	7.11	3.86	1.25
Ni^{+2}	0.00	0.00	0.00	0.00	0.00
HCO_3^-	151.51	610.09	142.22	414.00	----
pH	6.50	7.22	6.09	6.88	----

Sample = Andesine

ion	36 hr	112 hr	250 hr	512 hr
SiO_2	17.35	31.19	25.89	8.75
Al_2O_3	3.80	7.08	5.50	4.65
Na^+	36.07	42.26	7.60	2.48
K^+	11.70	12.26	2.08	3.58
Ca^{++}	52.45	57.42	29.07	19.73
HCO_3^-	175.50	198.86	55.38	77.70
pH	6.80	6.77	7.07	6.03

Sample = Labradorite

ion	38 hr	110 hr	275 hr	736 hr	2392 hr
SiO_2	31.05	24.70	23.77	13.80	9.60
Al_2O_3	0.98	0.00	8.75	0.83	1.57
Na^+	8.25	7.41	7.14	8.00	9.80
K^+	2.25	2.60	2.45	1.70	1.10
Ca^{++}	10.80	15.40	12.25	----	4.90
HCO_3^-	----	32.50	----	18.00	42.00
pH	----	5.80	6.16	6.57	7.00

Sample = Olivine

ion	30 hr	57 hr	147 hr	309 hr	737 hr	3137 hr
SiO_2	44.73	70.00	254.43	24.39	25.30	13.3
Al_2O_3	4.62	0.98	0.00	0.00	0.00	0.00
Mg^{++}	42.00	43.62	47.17	69.92	72.25	63.56
$Fe^{+2}+Fe^{+3}$	0.00	0.00	0.00	0.00	0.00	0.18
HCO_3^-	----	----	198.46	307.89	464.00	77.30
pH	7.23	7.76	7.97	7.67	7.21	7.55

Sample = Magnetite

ion	30 hr	68 hr	140 hr	305 hr	766 hr	2364 hr
$Fe^{+2}+Fe^{+3}$	2.36	2.44	1.45	1.75	1.24	0.93
HCO_3^-	106.00	102.50	187.80	72.47	14.11	13.56
pH	6.97	6.89	6.29	6.97	5.73	6.64

Sample = Augite

ion	30 hr	57 hr	147 hr	309 hr	737 hr	3137 hr
Si	25.04	529.20	250.20	176.40	78.55	15.10
Al_2O_3	0.00	0.00	0.00	0.00	0.00	0.00
Na^+	0.00	0.00	0.00	0.00	0.00	0.00
K^+	1.05	1.55	0.00	0.00	0.00	0.00
Ca^{++}	36.99	44.95	56.70	51.69	49.38	22.22
Mg^{++}	0.00	0.00	0.00	0.00	0.00	0.00
$Fe^{+2}+Fe^{+3}$	3.92	0.00	0.80	1.12	0.00	0.18
HCO_3	----	----	----	215.40	132.92	35.55
pH	7.60	----	7.65	7.40	6.62	6.75

TABLE 20

X-ray Data for Calcite

A	B
2.996	3.035
2.473	2.495
2.267	2.285
2.088	2.095
1.988	1.927
1.904	1.913
1.875	1.875
1.599	1.626
1.475	1.473

A: Calcite formed on glass sample as a result of the alternate wetting and drying experiments

B: Calcite reported by Swanson and Fuyat, NBS Circular 539, 51(II), 1953. (ASTM 5-0586)

APPENDIX C

APPARATUS FOR ALTERNATE WETTING AND DRYING EXPERIMENTS

The instrument constructed for these experiments automatically wet and dryed samples in cycles of eight minutes. It consists of a water reservoir, a microswitch driven by a cam, a solanoid valve, three infrared 250 watt lamps, three stainless steel sprinklers, four valves and three paper-beakers that serve as sample containers. The cam driven microswitch energizes the solanoid valve (normally closed) for a period of eighteen seconds during which distilled water flows through the paper beakers wetting the samples uniformally from the sides and bottom. The heated upper surface of the sample is thus soaked from below and splattering is avoided.

The infrared heating lamps are mounted above the samples at a distance that ranges between 3 to 5 cm. The exact distance is adjusted for every sample so that it dires completely in every cycle. An aluminum foil with a hole of a diameter somewhat smaller than that of the paper beaker is placed on each beaker to prevent its burning. The lamps and an electric clock are connected in parallel to the motor that drives the cam so that any failure in electricity would stop the operation of the whole system, and the clock records the time the apparatus is not functioning. A schematic diagram of the water in Figure 15 and a schematic diagram of the electronic circuit is described in Figure 16.

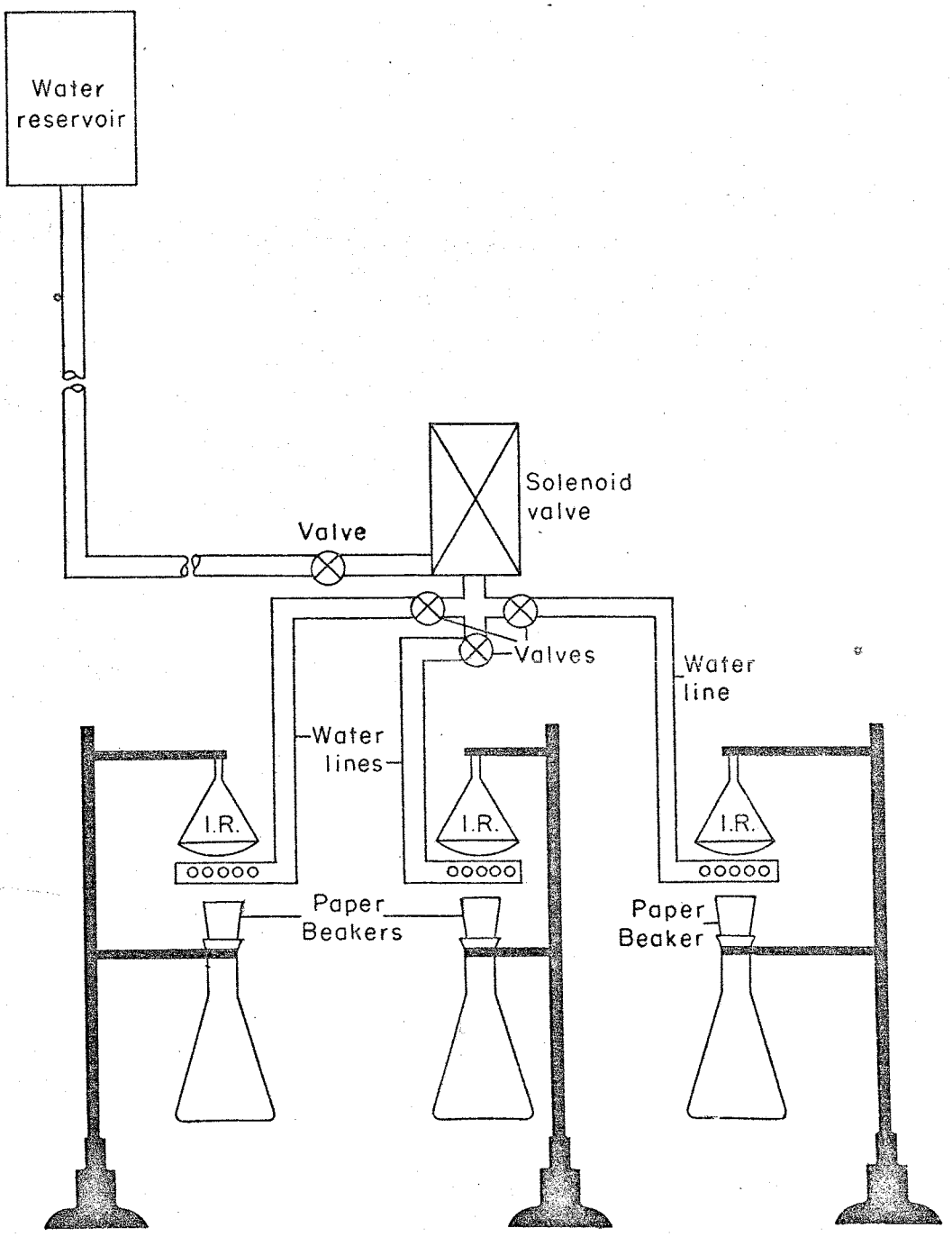

FIGURE 15
Schematic diagram of the water system.

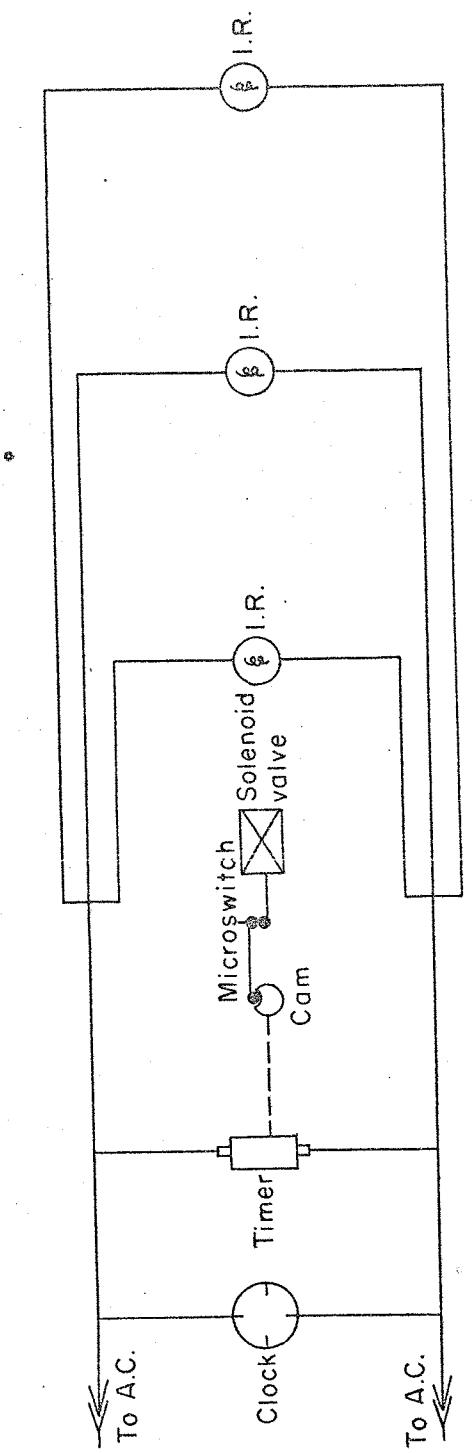

FIGURE 16
Schematic diagram of the electronic circuit

REFERENCES

Anderson, D. H., and H. E. Hawkes, 1958. Relative mobility of the common elements in weathering of some schists and granite area, Geochim. et Cosmochim. Acta, 14, 204.

A omine, S., and K. Wada, 1962. Differential weathering of volcanic ash and pumice resulting in formation of hydrated halloysite, Am. Min., 47, 1024.

Aristarain, L. F., 1970. Chemical analysis of caliche profiles from the high plains, New Mexico, Jour. of Geol., 78, 201.

Augustithis, S. S., and Otteman, 1966. Ondiffusion rings and spheroidal weathering, Chem. Geol., 1, 201.

Azároff, L. V., and M. T. Buerger, 1958. The Powder Method in x-ray Crystallography, McGraw-Hill Book Company Inc., New York.

Bates, T. F., 1962. Halloysite and gibbsite formation in Hawaii, Proc. Nat. Conf. Clays and Clay Minerals, 9, 307.

Bennett, H., and W. G. Hawley, 1965, Methods of Silicate Analysis, second edition, Academic Press. Inc., London and New York.

Berner, R. A., 1969. Goethite stability and origin of red beds, Geochim. et Cosmochim. Acta, 33, 220.

Bretz, J. H., and L. Horbert, 1949. Caliche in southeastern New Mexico, Jour. of Geol., 57, 491.

Barington, R. S., and D. C. May, 1958. Handbook of Probability and Statistics with Tables, McGraw-Hill Book Company Inc., New York.

Burkett, D. H., 1970. Experimental alteration of basaltic glass in aqueous environments, Thesis, Florida State University.

Burkett, D. H., R. B. Scott, and J. D. Leaird, 1970. Experimental alteration of basaltic glass in low temperature aqueous environments, U. S. G. S. annual meeting.

Carslaw, H. S., and J. C. Yaeger, 1970. Conduction of Heat in Solids, second edition, Oxford at the Clarendon Press.

Correns, C. W., 1961. The experimental weathering of silicates, Clay Min. Bull., 4 (26), 249.

Craig, D., and F. C. Loughnan, 1964. Chemical and mineralogical transformation accompanying the weathering of basic volcanic rocks from New South Wales, Aust. Jour. Soil. Science, 2, 218.

Dennen, W. H., and P. J. Anderson, 1962. Chemical changes in incipient rock weathering, Geol. Soc. of Am. Bull., 73, 375.

DeVore, G. W., 1958. The surface weathering of feldspars as an influence on their decomposition products, Proc. Nat. Conf. Clay and Clay Minerals, 6, 27.

Dixon, W. J., and F. J. Massey, 1957. Introduction to Statistical Analysis, McGraw Hill, Book Company, New York.

Douglas, R. W., and T. M. El-Shamy, 1967. Reactions of glasses with aqueous solutions, Jour. of Am. Cer. Soc., 50 (1), 1.

Eitel, W., 1958. Structural Conversions in Crystalline Systems and their importance for Geological Problems, Geol. Soc. of Am. Special Paper, No. 66.

Eyles, V. A., 1952. The composition and origin of the Antrim laterites and bauxites, Mem. Geol. Surv. N. Ireland.

Fields, M., and L. D. Swindale, 1954. Chemical weathering of silicates in soil formation, New Zealand Jour. Sci. and Technol., 366, 400.

Friedman, I., R. L. Smith, and W. D. Long, 1966. Hydration of natural glass and formation of perlite, Geol. Soc. of Am. Bull., 77, 323.

Gile, L. H., 1966. Cambic and certain noncambic horizons in desert soils of southern New Mexico, Soil Sci. Soc. Am. Proc., 30, 773.

Gile, L. H., J. W. Hawley, and R. B. Grossman, 1970. Guidebook, Soil-Geomorphology field Conf. Soil Sci. Soc. of Am., 51.

Goldich, S., 1938. A study in rock weathering, Jour. of Geol., 46, 17.

Graham, E. R., 1949. The plagioclase feldspars as an index of soil weathering, Soil Sci. Soc. Proc., 300.

Grim, R. E., 1953. Clay Mineralogy, McGraw-Hill Book Company, New York.

Harris, R. C., and J. A. Adams, 1966. Geochemical and mineralogical studies on the weathering of rocks, Am. Jour. of Sci., 264, 146.

Hauser, E. A., and H. H. Reynolds, 1939. Alteration of glasses to montmorillonite, Am. Min., 24, 590.

Hawley, J. W., 1965. Geomorphic surfaces along the Rio Grande Valley from El Paso, Texas to Caballo Reservoir, New Mexico, N. M. Geol. Soc. Guidebook, Southern New Mexico, II, 188.

Hawley, J. W., and L. H. Gile, 1966. Landscape evolution and soil genesis in the Rio Grande region, southern New Mexico, Guidebook, 11th annual field conference, Rocky Mountain section, Friends of the Pleistocene.

Hawley, J. W., 1967. K/Ar ages of the cenozoic basalts in Dona Ana county, New Mexico, N. M. Geol. Soc. Guidebook, Defiance-Zuni Mt. Taylor region, 226.

Hawley, J. W., and F. E. Kottlowski, 1969. Quaternary geology of the south-central New Mexico border region, N. M. Bur. Min. Min. Resources, Spec. Paper, Circ. 104, 116.

Hay, R. L., 1960. Rate of clay formation and mineral alteration in a 4000 year old volcanic ash soil on St. Vincent, B. W. I., Am. Jour. of Sci., 25, 354.

Jay, R. L., and B. F. Jones, 1971. Weathering of basaltic tephra on the Island of Hawa ii, Unpublished preprint.

Helgeson, H. C., Brown, T. H., and R. H. Leeper, 1969. Handbook of Theoretical Activity Diagrams Depicting Chemical Equilibria in Geological Systems Involving an Aqueous Phase at One Atom and 0° to 300°C, Freeman, Cooper, and Comp.

Helgeson, H. C., 1969. Thermodynamics of hydrothermal systems at elevated temperatures and pressures, Am. Jour. of Sci., 267, 729.

Helgeson, H. C., 1971. Kinetics and transfer among silicates and aqueous solutions, Geochim. et Cosmochim. Acta, 35, 421.

Hemin, S., and G. Pedro, 1957. The laboratory alteration of rocks, R. C. Acad. Sci., Paris, 245, 1451.

Hoffer, J. M., 1969. Volcanic history of the Black Mountain - Santo Tomas basalts, Potrillo volcanics, Dona Ana County, New Mexico, N. M. Geol. Soc. Guidebook, Northern Chihuahua, Mexico, 107.

Hoffer, J. M., 1971. Mineralogy and petrology of the Santo Tomas - Black Mountain basalt field, Potrillo volcanics, south-central New Mexico, Geol. Soc. of Am. Bull., 82, 603.

Huang, W. H., and W. D. Keller, 1970. Dissolution of rock forming minerals in organic acids: simulated first stage weathering of fresh mineral surfaces, Am. Min., 55, 2076.

Hudec, P. P., and J. R. Dunn, 1966. "Order water" molecular pressure offer new clues to rock failure, E/MJ., 167(7), 92.

Jenny, H., 1931. Behavior of potassium and sodium during the process of soil formation, Missouri Agr. Exp. Sta. Research Bull., No. 162.

Johnson, J. R., R. H. Bristow, and H. H. Blaw, 1951. Diffusion of ions in some simple glasses. Jour. of Am. Ceramic Soc., 34(6), 165.

Keller, W. D., 1957. The Principles of Weathering, second edition, Lucas Bros., Columbia, Missouri.

King, W. E., J. W. Hawley, J. W. Taylor, and R. P. Wilson, 1971. Geology and ground-water resources of central and western Dona Ana county, New Mexico, N. M. Bur. Min. Min. Resources, Hydrological Report, No. 1.

Kottlowski, F. E., 1958. Geological history of the Rio Grande near E. Paso, West Texas Geol. Guidebook, Field Trip.

Kottlowski, F. E., 1960. Reconnaissance geologic map of the Las Cruces thirty-nine quadrangle, N. M. Bur. Min. Min. Resources, Geol. Map, No. 14.

Krumbein, W. C., and F. A. Graybill, 1965. An Introduction to Statistical Models in Geology, McGraw-Hill Book Company, New York.

Kuno, H., K. Yamasaki, C. Iida, and K. Nagashima, 1957. Differentiation of Hawaiian magmas, Japanese Jour. Geol. Geography, 28, 179.

Laves, F., and S. Hafner, 1956. Ordnung/Unordnung and Ultrarotabsorption, I (Al, Si) - Verteilung in Faltspaten, Zs, f. Krist., 108, 52.

Lofgren, G. 1970. Experimental devitrification rate of rhyolites glass, Geol. Soc. of Am. Bull., 81, 553.

Loughnan, F. G., 1969. Chemical Weathering of the Silicate Minerals, Am. Elserier Publishing Company Inc.

Lyle, A. K., 1943. Theoretical aspects of chemical attack of glasses by water, Jour. of Am. Ceramic, Soc. 26(6), 201.

MacKay, A. L., 1960. β-ferric oxyhydroxide, Am. Min., 45, 454.

Manning, G., 1955. Laboratory weathering of feldspars and investigations of cations content of stream draining on essentially monolithic terrain, Thesis, Colorado School of Mines.

Martin, P. S., 1964. Pollen analysis and the full-glacial landscape, The Reconstruction of Past Environments.

Martin, P. S., and P. J. Mehringer, 1965. Pleistocene pollen analysis and biogeography of the southwest, The Quaternary of the United States, Princeton Univ. Press.

Marshall, C. E., 1964. The Physical Chemistry and Mineralogy of Soils, Vol. 1, Soil Materia, John Wiley and Sons, Inc., New York.

McLaughlin, R. J. W., 1955. Geochemical changes due to weathering under varying climatic conditions, Geochim. et Cosmochim. Acta, 8, 109.

Morey, G. W., and W. T. Chen, 1955. The action of hot water on some feldspars. Am. Min., 40, 996.

Nernst, W., 1911. Theoretical Physical Chemistry, sixth edition, London.

Nicholls, G. D., 1963. Environmental studies in sedimentary geochemistry, Sci. Prog., London, 51, 12.

Noble, D. C., 1957. Sodium, potassium and ferric ion content of some secondary hydrated natural silicic glasses, Am. Min., 52, 280.

Norton, F. H., 1941. Hydrothermal formation of clay minerals in the laboratory, Am. Min., 26, 1.

Parker, A., 1970. An index of weathering for silicate rocks, Geol. Mag., 501.

Pedro, G., 1964. Alteration geochimique des rocks, Annls. Argron., 15, 2.

Polynov, B. B., 1937. The Cycle of Weathering, Thos. Murby. London.

Reeves, C. C., 1970. Origin, classification and geologic history of caliche on the southern high plains, Texas and eastern New Mexico, Jour. of Geol., 78(3), 352.

Reeves, C. C., 1971. Relations of caliche to small natural depressions southern high plains, Texas and New Mexico, Geol. Soc. of Am., 82, 1938.

Reesman, A. L., and W. D. Keller, 1968. Aqueous solubility of high alumina and clay minerals, Am. Min., 53, 929.

Reiche, P., 1943. Graphic representation of chemical weathering, Jour. of Sed. Pet., 13, 58.

Reynolds, S. E., 1956. Climalogical Summary New Mexico Precipitation 1894-1954. State Engineer Office, Technical report, No. 6.

Renault, J. R., 1970. Major-element variation in the Potrillo,

Carrizozo and McCartys basalt fields, New Mexico, N. M. Bur. Min. Min. Resources, Cir., No. 113.

Robinson, W. G., 1949. Soils, their Origin, Constitution and Classification. Thomas Murby Company, London.

Ruhe, R. V., 1967. Geomorphic surfaces and surficial deposits in southern New Mexico, N. M. Bur. Min. Min. Resources, Memoir, No. 18.

Ruxton, B. P., 1968. Measures of the degree of chemical weathering of rocks, Jour. of Geol., 76, 518.

Sherman, G. D., 1949. Factors influencing the development of lateritic and laterite soils in the Hawaiian Islands, Pac. Sci., 3, 307.

Sherman, G. D., 1952a. The titanium content of Hawaiian soils and its significance, Proc. of Am. Soil Soc., 16, 15.

Sherman, G. D. 1952b. The genesis and morphology of the alumina-rich laterite clays, Clay and laterite genesis, Am. Inst. Min. Met., 154.

Smyth, C. H., 1913. Jour. of Geol., 21, 105.

Sun, Ming-Shan, 1957. The nature of iddingsite in some basalts of New Mexico, Am. Min., 42, 525.

Swift, H. R., 1945. Some experiments on crystal growth and solution in glasses, Jour. of Am. Ceramic Soc., 30 (6), 165.

Vanden Heuvel, R. C., 1966. The occurrence of sepiolite and attapulgite in the calcareous zone of a soil near Las Cruces, N. M., Clay and Clay Minerals, Proceedings of the 13th National Conference on Clay and Clay Minerals.

Volborth, A., 1963. Total instrumental analysis of rocks, Nev. Univ. Mackay School Mines, Rept. 6.

Whittaker, E. J. W., and Munt, R., 1970. Ionic radii for use in geochemistry, Geochim. et Cosmochim. Acta., 34, 945.

Wolff, W., 1967. Weathering of Woostock granite near Baltimore, Maryland, Am. Jour. of Sci., 265, 106.

Wollast, R., 1967. Kinetics of the lateration of K-spar in buffered solutions at low temperatures, Geochim. et Cosmochim. Acta., 31, 635.

This thesis is accepted on behalf of the faculty of the Institute by the following committee:

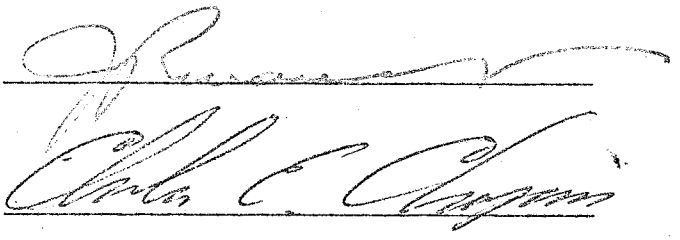

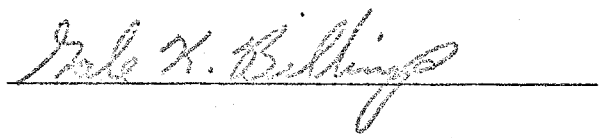

Date